2017

An investigation into the response of a modular pontoon system to wave loading

Gathergood, G.

Gathergood, G. (2017) 'An investigation into the response of a modular pontoon system to wave loading', The Plymouth Student Scientist, 10(1), p. 239-280.
http://hdl.handle.net/10026.1/14145

The Plymouth Student Scientist
University of Plymouth

*The Plymouth Student Scientist, 2017, **10**, (1), 239-280*

An investigation into the response of a modular pontoon system to wave loading

Graham Gathergood

Project Advisor: Martyn Hann, School of Marine Science and Engineering, Plymouth University, Drake Circus, Plymouth, PL4 8AA

Abstract

This project involves investigating the response of a modular pontoon system when put under wave loading. In addition, this report also hopes to establish a point at which the movement of a pontoon due to waves will cause the pontoon to be considered unsuitable for use. This research draws upon previous work conducted within the field and expands upon it using physical modelling. In this case the modelling comprises of a modular pontoon being subjected to waves with a range of frequencies and amplitudes. Thorough analysis of results obtained from this determined that under higher frequency waves the movement response of a modular pontoon is less than that when under low frequency waves. In addition, a recommended value for the slope of a modular pontoon of 1 in 7.5m was defined as the steepest allowable gradient for a modular pontoon before it should be considered unsafe for use.

1 Introduction

Modular Pontoons are used all over the world in many situations, mainly with respect to docks, floating walkways or offshore platforms. They are used commonly in temporary works as they are both easy to install and uninstall as well as being easy to adapt into different shapes and sizes depending on the usage. These systems are generally used in areas with little to no wave action, such as lakes, rivers and calmer areas of coastline. However, there is often a need for such platforms in areas where the water surface cannot be guaranteed to be calm. If it was the case where a modular pontoon was positioned in an area with a more active sea state, it must be suitable for use. The modular pontoon cannot be said to be fit for purpose unless the gradient, which it is likely to reach during its use, is known. As these pontoons are used by the public this gradient is likely to be required to be more gradual than if it were an industrial application.

The purpose of this project is to examine the relationship between the movement of a modular pontoon structure and the wave conditions to which it is subjected. A secondary aim of this report is to establish the maximum gradient a modular pontoon may reach under various wave conditions and under what conditions it would be considered to be unsuitable for public use.

The reaction of the pontoon surface will be examined through the use of a physical model. Using the coastal basin available at Plymouth University a model pontoon will be tested. This model will be subjected, under controlled conditions, to a spectrum of waves with various amplitudes and frequencies. The movement of the pontoon surface will then be recorded through the use of qualisys sensors. Data attained from these sensors will be analysed and compared to data obtained from the waves. This will aid in the determination of how a modular pontoon would respond to various wave conditions. Additionally, this data will be used in order to calculate the gradients which would be expected to occur upon the pontoon.

In basic terms, it is expected that the modular pontoons would respond to the induced waves simply by mimicking the variation in the water surface level. It is not known, however, whether this will hold true for all frequency and amplitude values. It is also unknown as to what effect the properties of the pontoon will have upon the amplitude of movement; it is suspected that it may suppress or dampen any movement caused. In term of the achieved gradient, it is expected that the higher amplitude waves will result in steep gradients. How the wave frequency will affect pontoon movement is not known at this time and will be investigated.

This project is partitioned into various sections to explain how the investigation was undertaken. This report will initially discuss the theory and background literature involved throughout the experiment. Following this the experimental methodology used to conduct the physical testing will be listed. The data analysis techniques used to better understand this data will then be summarised and results tabulated and represented graphically. The results will then be discussed specifically with respect to real world relevance as well as the application, deployment and use of modular pontoon systems. Finally, conclusions drawn will be summarised at the end of the report with supporting information, not nested within the report, located within the appendices.

2 Literature Review

For the purposes of this project it was necessary to research and analyse a variety of topic area to develop a suitable understanding of the project. These sources ranged from books and product specifications to previous studies and journal articles. A summary of these sources and relevant information gained is discussed below.

2.1 Modular Pontoons and Uses

Modular pontoons are a form of pontoon system widely used in industry due the versatility and adaptability inherent with their particular design. Unlike regular concrete or steel pontoons, which are often comparatively large and only suitable for custom sizes, a modular pontoon system is made up of several similar or identical interlocking smaller pontoon modules.

Modular Pontoons, due to the variety of configurations which can be achieved, can be used in an equally large variety of situations. Some example applications in which modular pontoons have been utilised are discussed below.

2.1.1 Temporary Works

Due to the ability to form modular pontoons into any required layout they are often deployed as cost effective access platforms in enabling or temporary works projects. Repair works to a bridge pier, for example. The temporary pontoon could be assembled to surround the bridge pier itself without the need to use large pontoons, which may not fit around the bridge pier correctly, introduce increased health and safety risks, or may block the navigable channel.

2.1.2 Piers and jetties

By using speciality pontoon modules, it is possible to further expand upon the versatility of the modular pontoon system. Modules like those sold by Versadock (2016) such as the V-Float allow storage of light vessels on deck. For this reason, modular pontoons are often used as small piers and jetties where light vessels and jet skis can be easily docked. Adjustable rollers can also be installed on the pontoon surface alongside a drysail system to allow manual docking and launching of smaller vessels.

2.1.3 Bridges and Walkways

A common use of modular pontoons is to create bridges and walkways. These may be for temporary use as part of a phased construction programme or as a cost effective semi-permanent alternative solution to a costlier traditional permanent structure. Pontoons are used in this capacity as they are relatively simple to deploy. Due to their inherent buoyancy and stability they can float well and are able to withstand heavy loads which may be transported across them. In construction projects, they may be used to transport or support heavy loads such as diggers. It has also been known for these pontoons to be used as they have been known to act as helipads within the military to create quick, easy to assemble landing zones.

2.1.4 Rafts

The modular pontoon system is also regularly used to create rafts. This is achieved by arranging the modules into a small pontoon and simply attaching a motor. These rafts can then be used in numerous situations depending on what is needed. The

main uses for modular pontoon rafts include allowing quick access to flooded areas and emergency evacuation.

For the purposes of this study the use of modular pontoon systems for beach landings and small piers has been investigated. When modular pontoons are used for this purpose, it is often in areas where wave action is not a dominant action, such as a lake or calm ocean conditions. This study aims to establish how a modular pontoon would react when subject to more turbulent wave conditions.

2.2 Waves

In order to tests the pontoon under various wave conditions it was first important to understand the many wave processes which would occur throughout the experiment.

Ocean waves are generated by wind on water; as the wind travels across a water surface, the effect of friction between the air and the water causes surface distortions. Surface tension then acts to restore the surface to its still water condition; this causes the surface to become rougher and hence more effected by friction between wind and sea. This is essentially how ocean waves are generated. (Kan, no date)

These waves can travel long distances; generally, wave height is lost with distance propagated but wave length and period are maintained. There are two main types of ocean waves; these are storm waves and swell waves. Storm waves typically occur in much higher frequency ranges than swell waves; however, they also tend to have greater wave heights. Low frequency waves travel quicker than high frequency and hence swells caused by a storm will reach the shore before the storm waves themselves. (Reeve, Chadwick, and Fleming, 2011)

As waves approach the shore they move from deep water conditions to transitional water conditions. The classification of whether a depth is classified as deep, transitional, or shallow water relies on the ratio of water depth to wave length (Kamphuis, 2010, p34). This requires a wavelength to be known. These water depth classifications and associated formulas for wavelength, given below, were taken from Wiegel (1964).

Deep Water,	$\frac{h}{L} > \frac{1}{2}$	$L_0 = \frac{gT^2}{2\pi}$
Transitional Water,	$\frac{1}{2} \geq \frac{h}{L} \geq \frac{1}{20}$	$L = \frac{gT^2}{2\pi}\tanh\left(\frac{2\pi h}{L}\right)$
Shallow Water,	$\frac{1}{20} > \frac{h}{L}$	$L = T\sqrt{gh}$

Where: L = wave length, L_0 = deep water wave length, T = wave period, g = gravity and h = water depth

Using the information above allows the wavelength of a wave to be calculated from only the water depth and the wave period. It is usually assumed initially that a wave operates in deep water, this assumption is then refined depending on the output water depth to wavelength ratio given by the equations.

The boundary between transitional and deep water conditions is the point at which the wave begins to be affected by water depth. It has been established that due to phenomenon such as shoaling and refraction, for example, that the interaction with

the sea bed is responsible for many coastal wave behaviours. Refraction occurs to the non-uniform bathymetry of the coastline (Kamphuis, 2010, p.128). As the wave celerity is partially dictated by water depth, when a wave front approaches the shore line different regions of the wave will decelerate at different rates due to the reduced depth in that area. This gives the effect that the wave is “turning” towards the shoreline; this effect can usually be seen clearly around headlands.

Shoaling occurs as the wave front travels towards the shoreline. In order to maintain energy despite the reducing water depth a wave will gain height (Shibayama, 2008, p53). This has the effect of reducing the wavelength of the wave and producing a taller sharper wave crest; this increase in wave height often leads to breaking.

The type of breaker and the location at which the breaking occurs is dependent upon the slope of the beach as well as the slope of the wave. A beach with a shallow slope and a steep incoming wave will be subject to spilling breakers. These spilling breakers occur when the crest of the wave moves faster than the wave as a whole. Spilling breakers begin well offshore and continue as the wave propagates shoreward. As the wave approaches the shore the wave height gradually decreases, the area in which this process occurs is known as the surf zone. For a shallow to intermediate beach slope subject to a less steep wave plunging breakers are likely to occur. These are the stereotypical wave where the crest is observed to curl over creating a “tunnel” of air within the breaking wave. Plunging breakers occur when moderately steep waves meet moderately steep beach slopes. Plunging breakers reduce in wave height much more rapidly meaning that the surf zone is a lot smaller. For very steep slopes the waves will break straight onto the beach as surging breakers, in this instance there would be no surf zone. The surf zone is a complex area of the coastal system where incoming waves and those reflected by the shoreline interact. (Reeve, Chadwick, and Fleming, 2011)

There are of course various behaviours which occur which are not related to the water depth such as diffraction and wave reflection both of which affect the nearshore behaviour of waves. Diffraction is a process where waves curve around obstructions by the radiation of wave energy. In the case of a breakwater the wave would diffract round to the shore side of the breakwater (Shibayama, 2008, p62). Visually this would be shown as radial wave front emanating from the point of the breakwater. As a consequence, the wave heights in the surrounding area would decrease to account for the dispersion of the embodied energy.

Wave Reflection is, as it sounds, simply when a wave front is reflected off a surface. Given the case of a vertical sea wall with a wave approaching with normal incidence, the reflected wave would have the same phase as the original wave, but would be travelling in the opposite direction. The reflected wave would also have reduced amplitude to account for any energy lost through transmission and dissipation. In the case when the angle of incidence is not normal to the vertical wall, the reflected wave will travel with the same angle as the approaching, but from the opposite side of the normal. The wave motion resulting from this, known as ‘clapotis gaufre’, is a diamond pattern of island crests which move parallel to the vertical sea wall as defined by Silvester (1974).

When in natural sea conditions it can be difficult to distinguish the various behaviours previously discussed. In the case of this study however the only behaviours which

need to be accounted for are shoaling induced by the beach slope and reflection off the back of the coastal basin.

2.3 Extreme Value Analysis – Peak Over Threshold and Annual Maxima

When constructing a pier, many factors need to be considered. These include, but are not limited to the cost of construction, materials used, the design life of the structure and the height of the pier. As such the extreme wave heights for the area should be known. This allows the pier to be designed so that it does not become unnecessarily submerged. An advantage to a floating pier, such as one comprised of modular pontoons, is that it will not become submerged due to its inherent buoyancy. Nevertheless, these extreme wave heights still need to be known to provide an insight into the behaviour of the waves at any given location and hence whether the floating pier will represent a suitable design solution. The wave heights are calculated using an extreme value analysis. This calculation method consists of reducing the data set such that it is composed of only the extreme values. This reduced data set can then be attributed to a cumulative distribution function. By finding a trend with this data values can be extrapolated for values outside the existing data set.

2.4 Pontoon System Investigations

Prior to carrying out this investigation it was important to find if any similar research papers or studies had been conducted previously. It was found that a limited number of papers shared similarities with the current study, although none of which were wholly relevant. The studies found were primarily numerical studies although some included aspects of physical modelling used for comparison and validation of output from the different models used. No relevant studies were identified which discussed any physical modelling in detail leading to the conclusion that no physical testing has been previously conducted for this subject area. The more relevant of the researched studies will be discussed.

Abul-Azm and Gesraha (2000) investigated a long rigid pontoon under oblique waves for the purpose of defining if a floating pontoon was a suitable alternative for protection from waves when in shallow water. This, unlike the current investigation, was investigated numerically. In this study, this numerical analysis is undertaken using eigenfunction expansions to calculate the forces upon the structure, the force transmitted through the body and the reflection coefficients under oblique waves. This is valid when assuming rigid body motions, however for the case of the modular pontoon structure the numerical approach would not be as straight forward.

Another similar study is also presented by Gesraha (2004). The study aims to explore the action of floating pontoons to oblique waves. The situation is explored with regards to wave scattering and radiation. Similar to his previous work an eigenfunction expansion solution is adopted and solved. Results here correlate with that given from previous studies.

Gao, Wang and Koh (2013) conducted a numerical study which aimed to establish how the inclusion of gill cells, compartments of a large pontoon structure with allow the passage of water through them, and flexible connectors could reduce the hydroelastic response of a large pontoon structure when under wave action. This particular study was interesting because the resulting hydroelastic deformation could cause the large pontoon to be unable to meet its serviceability requirements. A modular pontoon however, as used for the current study, would be less impacted by this deformation as the pontoon modules would be more adaptable to the constantly

changing surface level of the water. The method used by Gao, Wang and Koh (2013) to analyse this was, put simply, to model the large pontoon as a plate, and perform a finite element analysis across the pontoon to establish and solve the equations of motion. The study concludes that the use of gill cells beneath areas of maximum deformation is most effective in reducing the hydroelastic response of the large pontoon. It was decided that a similar numerical method would not suffice for the current study due to the nature of the connections between the pontoon modules of the modular pontoon.

Arguably one of the more relevant papers of those researched was the work carried out by Michailides, Loukogeorgaki and Angelides (2013). This investigated the optimum configuration of a modular floating structure when using flexible connectors. Unlike the previous studies, they used a "wet" analysis as opposed to a "dry" numerical analysis. By Loukogeorgaki et al (2012), a "wet" analysis is computationally more expensive than "dry", however output frequencies and calculated data better represent the real-world behaviour. They further explained that this is because "wet" analysis better emulates the interaction between the pontoon modules by mimicking their behaviour more closely to that seen in the physical world. This "wet" analysis included a frequency domain hydroelastic analysis as well as a genetic algorithm to determine the optimum configuration of the modular pontoon floating structure. The study determined, among other conclusions, that in order to minimise the vertical hydroelastic response a 2 x 2 pontoon arrangement was optimum for wave incidences of 0 and 45 degrees.

Further research and evaluation of the studies described above resulted in the belief that numerical analysis was not the optimal method to adopt with the modular pontoon investigation. This was due to the fact that the interaction between the various pontoon modules was of key importance. To accurately model this numerically it would have been necessary to perform "wet" analysis. This would have been too arduous to model accurately given the resources available. Instead it was decided that physical modelling would be more appropriate for the purposes of this study as this would enable measurements and numerical output which would be arguably of more relevance to real world applications.

2.5 Physical Modelling

Numerical modelling as used throughout the previous papers would have been a very useful tool for predicting and defining the movement exhibited by the modular pontoons instead of physical modelling which was chosen for the project. Physical modelling entails its own advantages and limitations. The main advantage to physical modelling is that many of the complex processes which occur within the nearshore zone cannot be accurately modelled numerically. This means any results gained from physical modelling are likely to be more replicable for real world applications, whilst a numerical approach may result in a rather reductionist model as not all factors could be accounted for. A physical model also enables many different data sets to be recorded from a single model, whilst a numerical model is only fit for a single purpose.

It is, of course, important to note that a physical model cannot really be carried out in full scale due to size restraints within the laboratory. This means that any model has be carried out at a reduced scale when compared to the full-size structure, known as the prototype. This reduced scale can be decided in several ways as, depending

upon what the model is to be used for; the model can be scaled to allow for geometric similarity, kinematic similarity as well as dynamic similarity (Hughes, 1993, P54-62). These allow for similarity of form, motion, and forces respectively. Geometric similarity simply means the ratios between the model dimensions and the prototype dimensions are equal. Kinematic and dynamic similarities refer to the ratios between velocities and forces respectively. (Chanson 1999)

The Buckingham π theorem (Buckingham, 1915), states that all basic parameters' dimensions can be grouped into five dimensionless parameters (known as π terms) each independent of another. These are the Froude (Fr), Euler (Eu), Reynolds (Re), Weber (We) and Sarrau-Mach (Ma) numbers. These, as laid out by Chanson (1999), are shown below:

$$Fr = \frac{V}{\sqrt{gL}}; \quad Eu = \frac{\rho V^2}{\Delta P}; \quad Re = \frac{\rho VL}{\mu}; \quad We = \frac{V}{\sqrt{\frac{\sigma}{\rho L}}}; \quad Ma = \frac{V}{\sqrt{\frac{E_b}{\rho}}}$$

Where: V = velocity, g = acceleration of gravity, L = length, ρ = fluid density, P = pressure, μ = dynamic viscosity of water, σ = surface tension of air and water, and E_b = bulk modulus of elasticity of water

Scale effects are induced for each of the π-terms which are not maintained between the prototype and the model (Chanson 2004). In the case of wave modelling, the free surface of the water means that the effect of gravity is important. Hence the ratio of the Froude number, the ratio of inertia forces to that of gravity, would be taken from Buckingham as the more critical parameter to maintain. The Froude number would be taken as the dominant criteria to satisfy as it is not possible to satisfy the Froude, Reynolds, and Weber terms simultaneously (Hamill, 2011, p369).

3 Methodology

Before the physical modelling could be conducted there were many questions which needed to be answered. This included the matter of making the model itself and establishing the waves which it would be subjected to. The coastal basin could then be set up to better suit the experiment, Qualisys sensors could then be fitted to the modular pontoon. Only following all of this could the physical modelling begin.

3.1 Choosing a Scale

In order to correctly construct a model and establish the waves to subject it to, it was first necessary to establish a suitable scale. The method of doing this, which was decided upon, was to base the scale of the model on the size of the waves which could be produced within the coastal basin. To do this the size of waves that a pontoon pier may include needed to be known. Performing a Peak over Threshold (POT) analysis on wave data from West Bay, a likely position for a modular pontoon pier in the UK, resulted in the 1 in 100 year wave height for this location. This procedure for this extreme value analysis follows.

3.1.1 Extreme Value Analysis

The extreme value analysis that was required was that of the inshore wave buoy data from West Bay; this data was attained from the Channel Coast Observatory (CCO) (GeoData Institute, 2016).

As part of the analysis the data set first had to be reduced to account for the flag given by the data set. The flag represents the condition of the wave buoy and the data at that time instance; not all data can be relied upon. The reduced data was then analyses using the method of Gottschalk and Krasovskaia (2002) for guidance.

Following this a threshold of 2.5m was chosen to give a representative reduced data set. This threshold was positioned such that only 120 independent storm events occurred throughout the duration of the data set. To ensure storm wave heights were due to independent storm events the minimum time interval between two peak values was taken to be 4 days. The wave data was too sizeable to be included within this report, however it can be found diagrammatically in Figure **3.1**. This shows the extents of the wave data in addition to the location of the threshold and the location of any peak values used.

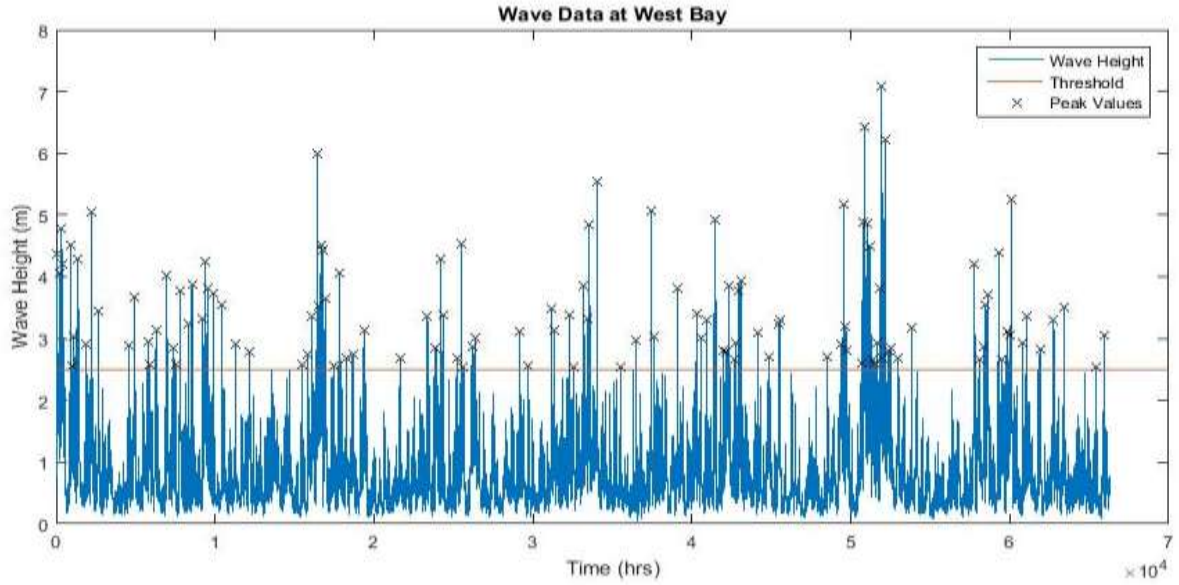

Figure 3.1 - Wave Data at West Bay

As this data set is comprised of maximum wave heights from independent storm events it can be represented as a cumulative distribution function (CDF). The data was checked for suitability with Gumbel, Weibull and Fréchet distributions. What follows are some basic calculations which were conducted to best represent the data points as a CDF. Firstly, the data was ranked in descending order. Following this the non-exceedance probability (*y*) for each wave height (*x*) within the data set was calculated.

$$P(X \geq x) = y = \frac{i}{N+1},$$

Where N = size of reduced data set, in this case N = 120

Following this the wave parameter, $g(x)$, and the reduced variate, $h(y)$, were calculated. The reduced variate remains constant across all three distributions, this is given below.

$$h(y) = -\ln(-\ln(y))$$

The wave parameter varies across the various CDFs. These wave parameters were calculated, following equations provided by Iglesias (2016), as detailed as below.

Gumbel: $g(x) = x$

Weibull: $g(x) = -\ln(\lambda - x)$

Fréchet: $g(x) = -\ln(x - \lambda)$

In these equations λ is a calibration parameter, which in this case is set to 2.5 and 8 for Fréchet and Weibull distributions respectively. The results of this are shown below for the Fréchet distribution in Figure **3.2** alongside a line of best fit to enable easier extraction of values. Similar figures for the Weibull and Gumbel distributions can be found in Appendix A.

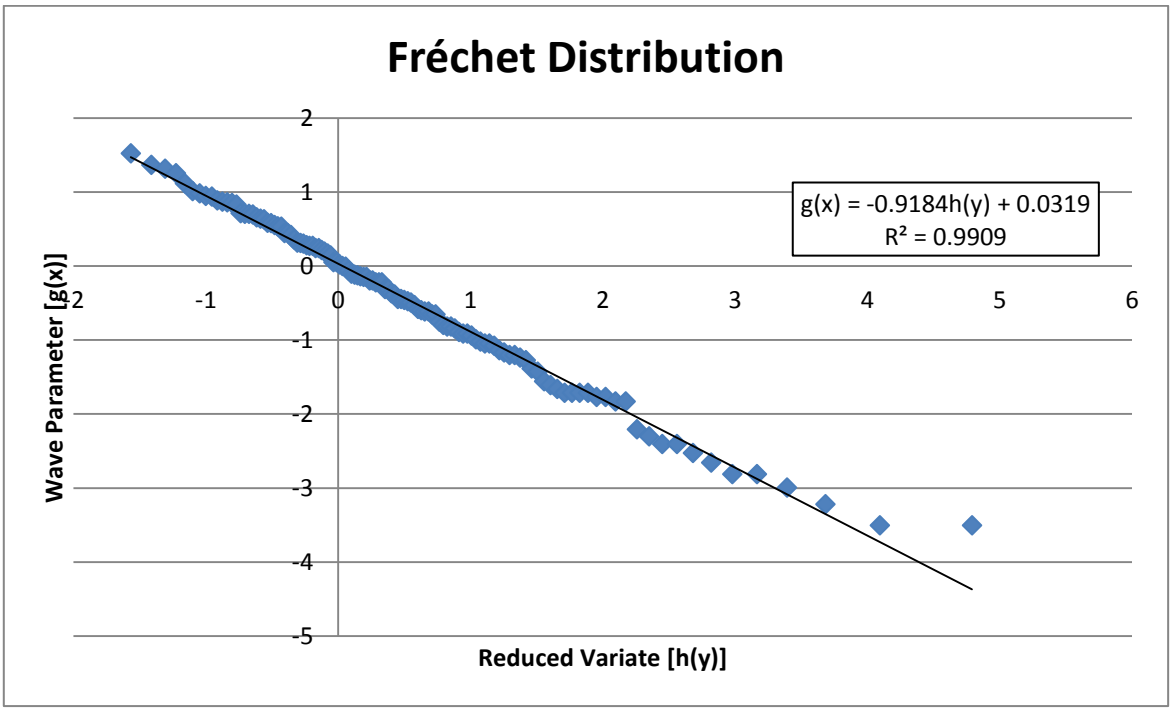

Figure 3.2 - Fréchet Distribution of Extreme Wave Heights

From the data, a Fréchet distribution was selected as this clearly represented the best data fit, the value of R^2 being significantly closer to unity. Following this, wave heights which correspond to certain return periods could be calculated. To do this the probability of exceedance (y) was calculated for each return period (T_r).

$$y = \frac{1}{T_r}$$

These probabilities of exceedance were then used to calculate a reduced variate which could be used in conjunction with the trend line from Figure **3.2** to obtain a value for the wave height.

$$h(y) = -\ln(-\ln(y))$$

$$g(x) = -0.9184 \times h(y) + 0.0319$$

$$H_s = e^{g(x)} + \lambda$$

The calculated wave heights are displayed in Table 3.1.

Table 3.1 - Extreme Wave Heights at West Bay

Return Period *(T_r, years)*	Probability of Exceedance *(y)*	Reduced Variate *h(y)*	Wave Parameter *g(x)*	Wave Height *(Hs, m)*
1:100	0.010	-1.527	1.434	**6.70**
1:50	0.020	-1.364	1.285	**6.11**
1:20	0.050	-1.097	1.040	**5.33**
1:15	0.067	-0.996	0.947	**5.08**
1:10	0.100	-0.834	0.798	**4.72**
1:5	0.200	-0.476	0.469	**4.10**
1:2	0.500	0.367	-0.305	**3.24**
1:1	1.000	11.513	-10.542	**2.50**

It should be noted that the 1:1 year wave height was technically not possible to calculate as it results in the need to take the natural log of 1 which is not calculable. Instead a number infinitesimally larger than 1 was used to gain a valid wave height output.

The calculated wave heights were used to gain a better perspective into the size of waves that the pontoon may experience and to thus inform a suitable scale. The 1:100 year wave height given in

Table **3.1** of 6.7m was used to decide the scale factor for the model. Strictly the coastal basin could produce a peak wave height of 0.32m, giving a 1:20 scale, however this could not be generated across the wave of frequencies required. The generation capacities of the coastal basin would have made it necessary to have a model with scale 1:200 to produce a wave height suitable for use across all frequencies. This model would have resulted in a model pontoon of insufficient size to be practical. In terms of manufacture it would have been too small, and hence fragile, to effectively work with. It would also have been more challenging to obtain meaningful results as the smaller pontoon modules would likely have induced scale effects as discussed in 2.5. Model effects would also be present as the pontoon would be too flexible and its behaviour across waves would not be representative of real sea state conditions.

It was decided therefore to adopt a 1:10 scale for the model. This would enable the pontoon modules to be a suitable size for manufacture; it also allowed the pontoon modules to have Qualisys sensors mounted upon them. Wave heights which were more similar to normal conditions, around 2.5m, would have ideally been modelled with the same scale factor. However, wave generation capacity was again a limiting factor which resulted in the choice to scale wave heights with a separate scale factor of 1:100.

It was judged that the loss of useful data due to the varying scale between model and waves would be less significant than that due to scale effects and model effect had the 1:200 scale been used. This is especially true given how the aim of this study is

simply to investigate the response of a modular pontoon structure. The extent to which the modular pontoon is subjected to wave conditions similar to that given by the extreme value analysis is almost arbitrary. It simply means that the wave conditions in the West Bay were too extreme to be modelled effectively within the wave basin. The wave conditions chosen will better reflect a calmer wave climate.

3.2 Model Making

Having established suitable scale, it was necessary to manufacture a model. It was decided that this model would be to simulate a modular pontoon pier construct which would be comprised of Versadock Single Float pontoon modules, which have a weight of 6.5kg and dimensions of 483 x 483 x 390mm. This pontoon module is. shown in Figure **3.3** below. The density of the full-size modules can be calculated to be 71kg/m³. For simplicity, the dimensions 50 x 50 x 40mm were used for the scale model.

Figure 3.3 - Single Float Pontoon Module, as made by Versadock (2016)

There were two aspects of the model which had to be decided upon. These were the pontoon model itself and the method of connection between them. Several methods of construction were considered however it was, frustratingly, more difficult that would be expected to produce a model which would accurately demonstrate the behaviours of the pontoon.

The initial choice to be made was whether to have the main pontoon module as a solid cube for simplicity, or to create a hollow cube. The hollow cube would have been an ideal choice if not for the difficulty in manufacture, especially given the budget for this project. Due to this reason the pontoon modules were modelled as solid cubes where the buoyancy would be maintained across model pontoon and full size. This buoyancy was difficult to replicate when producing a scale model as buoyancy does not scale linearly. After consideration of various materials, including balsa wood with a density of 160kg/m³ (Wood densities, no date) and polypropylene uniboard with density of 650kg/m³ (Plastics technical properties, no date), blue foam was settled upon as the material to use to manufacture the model. This material had a density of 52kg/m³ which is most similar to the modular pontoon blocks themselves and would therefore help to reduce any scale effects encountered. Although this material would technically be too buoyant for its desired use, it was reasoned that the weight of the connection method would counteract this. An example of one of these blue foam pontoon blocks is shown within Figure **3.4**.

Figure 3.4 - Blue Foam Pontoon Module

The choice to use blue foam for the models base material came with its own consequences however, as blue foam is not as sturdy as either plastic or timber. This meant that the connections between the pontoon modules were more difficult to construct, especially given the movement they would be required to endure. The connection points between the model pontoon modules needed to be able to replicate the behaviour of the joints used in real world situations. The main option considered was to laser cut a basic frame, which would then be attached to each pontoon module; this frame would then allow the modules to be connected via a pin joint in each corner. However, it was reasoned that an interlocking pin system would be too complex to manufacture given temporal and financial constraints. Following this an alternate method was derived, this was to connect the nexus of pontoon modules with strips of fabric. This fabric would be light enough that the pontoons buoyancy would not be adversely affected but would still mimic the effect of the pin joints within the full size modular pontoon and hence ensure the correct type of movement was exhibited.

Following the choice to use blue foam connected by fabric, a suitable fabric and adhesive had to be chosen. Peel ply was the first material which was considered but this did not bind well with any adhesive which resulted in the model coming apart when immersed in water. After some further review analysis and consideration sheet of cotton which would bind well with adhesive, and was strong enough to hold the model together under wave conditions was adopted. PVA was the first adhesive considered purely due to availability, however it was soon established it did not hold up when immersed for long periods of time. As the model modular pontoon was going to be getting wet, this would not have been a sensible choice. Instead, wood adhesive was adopted and through simulated testing was established to cope better under submerged conditions.

Having decided upon the materials there was the matter of establishing the type of connection which would best suit the model; two layouts of fabric considered. The former was fabric strips in a grid arrangement, to cover every join within the grid of pontoon modules. This option of pontoon connection is demonstrated in Figure 3.5.

Figure 3.5 - Connection Method 1 - Grid Arrangement

The latter option of module connection was to apply these fabric strips to the pontoon modules such that they were only covering the inside corners, and would hence act as pins. An example of this method of connection is shown in Figure 3.6.

Figure 3.6 - Connection Method 2 - Diagonal Arrangement

After testing the prototype connection methods shown in these figures it was revealed that the latter connection type allowed too much movement for the pontoon and caused it to be too fragile and so the grid arrangement was chosen. This gave the effect of hinges along the length of each joint of the pontoon, which although does not accurately reflect the pontoon system and how it functions in the real world, was the most viable that could be implemented with the available resources.

3.3 Coastal Basin Set-Up

In order for the coastal basin to be utilised effectively it was necessary to set up the basin properly. This required the set-up of the water depth as well as four wave gauges. The water depth was set to be 500mm as dictated by the operating software; thus enabling the wave paddles to accurately create the desired waves. This 500mm is accurate only to the nearest 5mm due to difficulties in accurately manipulating the water level using the pumping system; however, for the purpose of calculations it is assumed that the depth was exactly 500mm.

The pontoon was positioned in the centre of the basin such that the landside end of the pontoon was on the still water level drying line. This arrangement can be seen in the experimental layout in Figure **3.7**.

In reality, the pontoon could have run up the beach as far as allowable. For the model, due to its limited length, the pontoon had to be placed so as much of its length was in use on the water. In order to do this, it was decided that the pontoon should mimic a connection to a sea wall as is often done in real world applications.

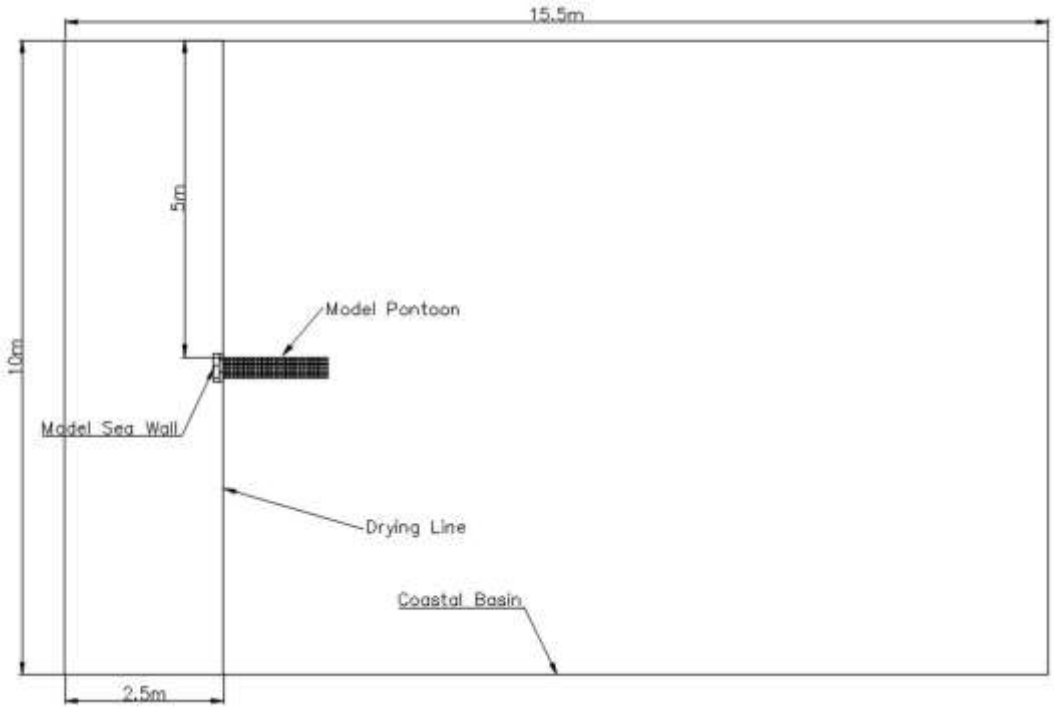

Figure 3.7 - Coastal Basin Layout

The method of doing this was to construct a small wall from loose bricks behind the pontoon to prevent it from being washed up the beach. The sea wall bracing also prevented the model pontoon from being washed up the beach slope by waves. However, there was nothing preventing the pontoon from being washed out into deeper water. To solve this problem the pontoon was tied back to a position behind the sea wall which prevented any movement. This solution can be seen pictorially in Figure 3.8.

Figure 3.8 - Sea Wall Bracing of Modular Pontoon

This allowed the pontoon to sway and move in relation to the motion of the waves, but the landside end was fixed in position. The result of this arrangement is that for

all intents and purposes the modular pontoon was moored against the sea wall as in some real-life situations.

The four wave gauges were positioned in front of, and alongside the pontoon. The number of gauges alongside the pontoon was limited by the shallow water depth. The aim of these wave gauges was to be able to know whether the wave paddles were generating the required waves correctly and to provide informational wave data at the same depth as the pontoon. This would allow easy comparison between the oscillations of the pontoon in comparison to the water level at any point. The arrangement of these wave gauges can be seen in the experimental layout in Figure **3.9** below.

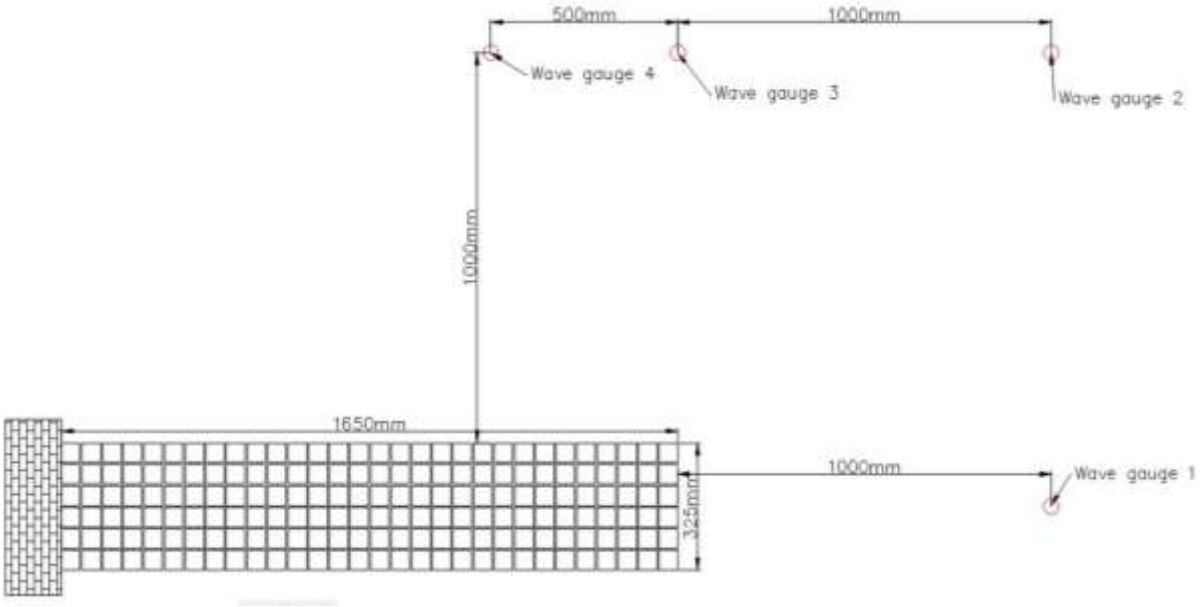

Figure 3.9 - Wave Gauge Layout

3.4 Qualisys

The Qualisys system employed operated as follows; several Qualisys cameras were positioned around the modular pontoon. The cameras aim was to locate sensors and track their movement; so with this in mind ten Qualisys sensors were added to the model. The sensors had to be attached to the pontoon at regular intervals and were loaded towards the offshore end of the pontoon as it was believed that the more useful movement data would be here rather than in the intertidal zone. Their positions are demonstrated within Figure **3.10**.

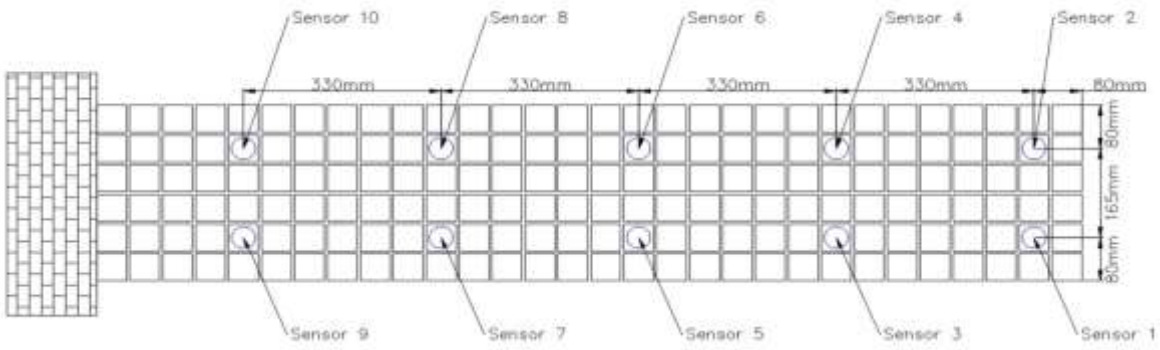

Figure 3.10 - Qualisys Sensor Layout

It was attempted to attach these sensors with double sided tape to reduce the load upon the pontoon. This proved to be ineffective given the nature of the testing as the tape was not suitable in damp conditions. Instead the sensors were connected to the pontoon modules using nails, which provided some additional weight, but it was assumed to not be significant enough to drastically affect any results.

3.5 Physical Modelling

Following the completion of this setup it was possible to begin the physical modelling itself. The testing comprised of testing the pontoon to a variety of wave frequencies whilst maintaining the amplitude at a set level. After deliberation, this was set as 0.01m amplitude, based upon the 0.0125m given by reducing the normal wave height of 2.5m by the 1:100 scale factor. The frequencies ranged the full range of the wave paddles going from 0.2Hz to 2Hz in steps of 0.05Hz. The same range of frequencies was also modelled for amplitude of 0.02m.

It terms of actually conducting the experiment it was simply a matter of starting the wave paddles and the Qualisys recording software for the duration of an experimental run; these both had to be started simultaneously. For the experiment, it was decided that each wave run would be three minutes in length. This was deemed enough time to get an accurate impression of the pontoons relative movement under the different wave conditions imposed upon it. To try and start each experimental run with as similar base conditions as possible it would have been ideal to allow the water within the coastal basin to settle before performing each run. This was not feasible due to time constraints; instead the basin was given two minutes to allow the water to settle to an allowable level before each run.

4 Data Analysis

For the purposes of the experiment several sets of calculations were required to be carried out. The calculations and data analysis were not just based upon the experimental results, but also on background theory and knowledge to gain predicted values for purposes of comparison. These were all required to gain a complete understanding of the accumulated data. This section of the report details and discusses the approaches taken to complete the numerical analysis throughout the project.

4.1 Wave Gauge Data

Calculations were performed upon the information gained from the wave gauges. This was to allow data attained from them to be directly compared to the output by the Qualisys sensors. There were two main sets of calculations carried out for the wave gauge data, the first of which were the calculations of the expected maximum wave height. This wave height would not simply be equal to twice the input amplitude due to the effect of shoaling as discussed within Section 2.2. The second was the determination of the maximum wave height recorded as well as the maximum and average amplitudes of the waves which were generated.

It should be noted that these wave gauges output data to 8 decimal places; hence the greatest possible error for each reading is only 5 nanometres. Whether the data is actually accurate to this degree is another matter entirely and is to be discussed within Section 6.1. The wave gauges output data with a sampling rate of 128Hz.

4.1.1 Expected Wave Height Due to Shoaling

The wave heights which were created using the wave paddles will only have maintained their characteristic properties whilst in water of constant depth. For the coastal basin, this is the area where the depth is equal to 500mm. As the depth reduces at the beach slope, the wave height changes due to shoaling and hence the maximum wave will be greater than expected based on the input conditions. Using Airy wave theory (Schwartz, 1984) the new wave height due to shoaling can be calculated. This is done using the formulae below. Given the sinusoidal nature of the utilised waves, calculations were completed in terms of amplitude for convenience:

$$K_s = \left(\frac{2\cosh^2(kh_i)}{\sinh(2kh_i)+2kh_i}\right)^{\frac{1}{2}}, \qquad \text{(Schwartz, 1984)}$$

Where: K_s is the shoaling coefficient, k is the wave number $\left(\frac{2\pi}{L}\right)$ and h_i is the depth at the wave gauge

$$A_i = A_0 K_s,$$

Where: A_i is the wave amplitude at the wave gauge and A_0 is the wave amplitude in deep water.

In order to utilise these formulae, the wavelength must be calculated. Taking an example experimental run with frequency 0.4Hz and amplitude 0.01m, and following the method set out within Section 2.2, gives the following.

$$h = 500mm, \qquad T = \frac{1}{0.4} = 2.5s$$

Assuming deep water:

$$L_0 = \frac{gT^2}{2\pi} = 9.76m$$

$$\frac{h}{L_0} = 0.051, \qquad hence\ transitional$$

Assuming transitional water:

$$L = \frac{gT^2}{2\pi}\tanh\left(\frac{2\pi h}{L}\right)$$

Solving for L gives L = 5.24m

$$\frac{h}{L} = 0.095, \qquad hence\ transitional$$

From then onwards for calculations it is simply a matter of following the equations to gain the shoaling coefficient. The shoaling coefficient would be calculated for each of the 4 wave gauges using the different depths at each for h_i. This was then used to calculate the amplitude due to shoaling at each of the wave gauges. This was repeated for each of the frequencies used throughout the experiment for both amplitudes used.

To continue the above numerical example, for wave gauge 1, which has a still level water depth of 0.275m, the following would be performed.

$$K = \frac{2\pi}{5.24} = 1.2$$

$$K_s = \left(\frac{2 \times \cosh^2(1.2 \times 0.275)}{\sinh(2 \times 1.2 \times 0.275) + 2 \times 1.2 \times 0.275}\right)^{\frac{1}{2}} = 1.28$$

Hence,

$$A_i = A_0 K_s = 0.01 \times 1.28 = 0.013m,$$

The result of the calculations for each of the wave gauges across both amplitudes and the full range of frequencies are displayed graphically to allow comparison to the exhibited amplitudes on the figures within Appendix B.

4.1.2 Maximum and Average Amplitudes from Wave Gauges

Another important aspect of the data analysis was the actual amplitudes induced by the wave paddles upon the modular pontoon. This was measured through the wave amplitudes experienced by the corresponding wave gauges alongside the pontoon.

The data output from these wave gauges was given in terms of water level for each wave gauge and was sampled at a rate of 128Hz across the course of the experiment. Matlab, a numerical computation software tool, was used to analyse the data. Within Matlab the following numerical procedures were used. The full data set for wave gauge 1 under 0.25Hz and 0.01m amplitude waves is given in Figure **4.1**.

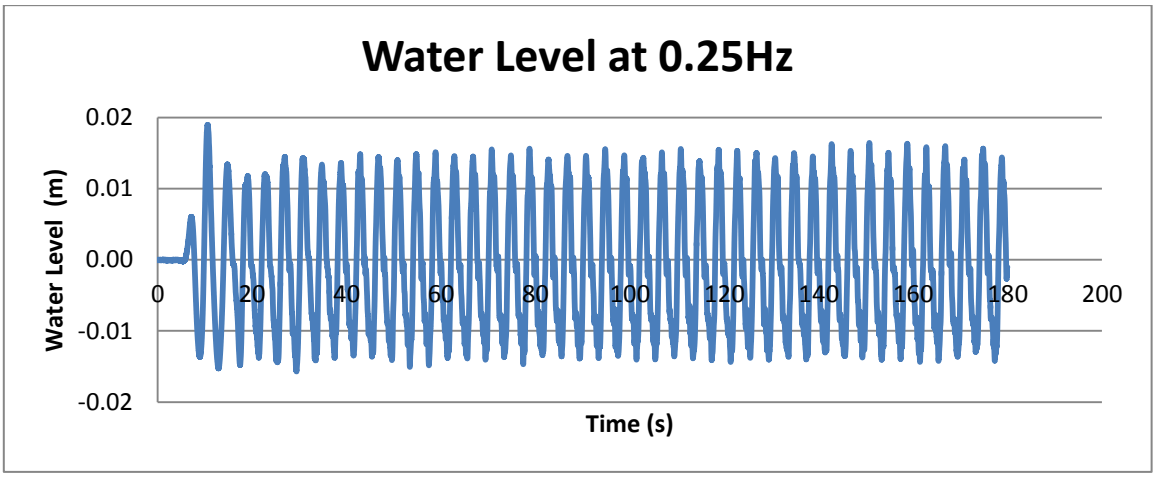

Figure 4.1 - Water Level at Wave Gauge 1

To calculate the average amplitude of the waves experienced from a wave gauge the wave data was analysed between two points. These were a time point part way into the experiment (such that the waves had settled into a consistent pattern, rather than being analogous due to wave set up) to a point 25 waves later. This number of waves was used as the length of the experimental run limited how many full waves could be completed. This reduced data set for the same experimental run and gauge is shown in Figure **4.2** below.

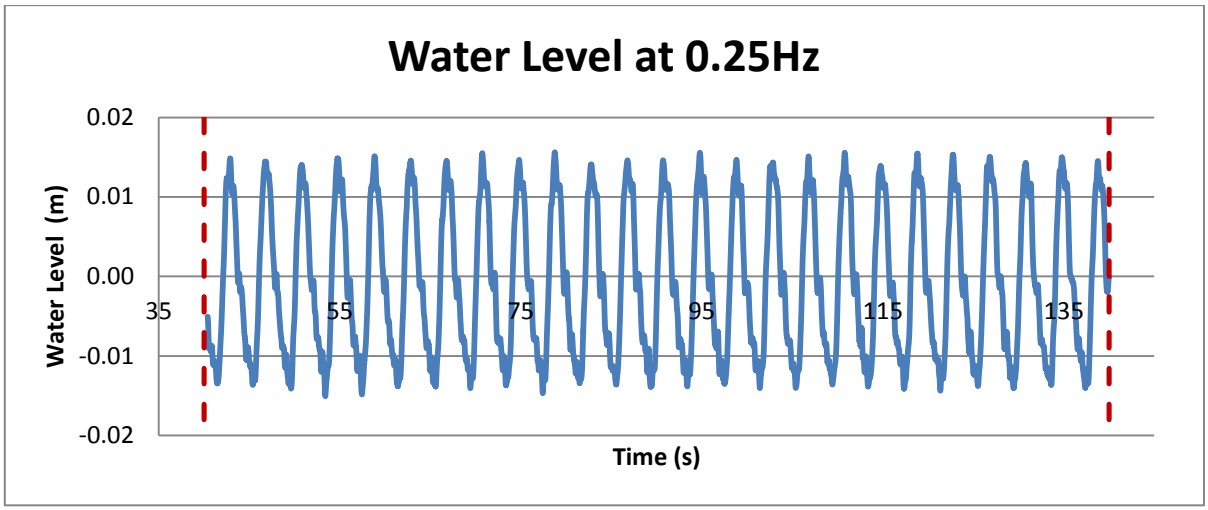

Figure 4.2 - Reduced Water Level Data Set

Within this range of time the data was reduced to a set of wave peaks and their specific locations, these peaks are identified within Figure **4.3**.

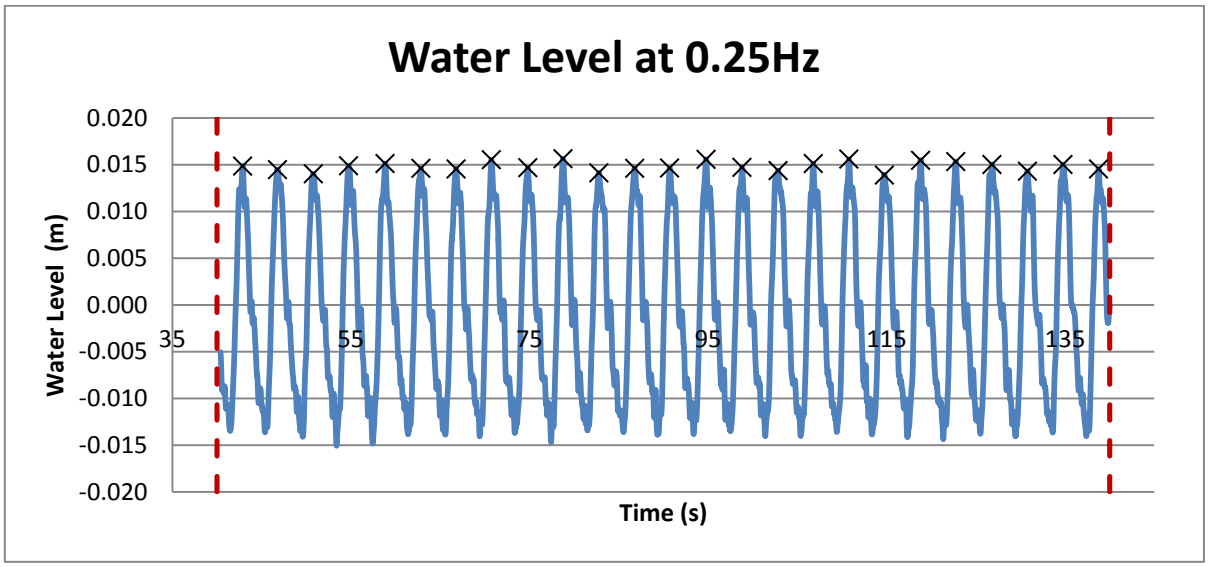

Figure 4.3 - Water Level Peak Locations

The average amplitude was defined as simply the average of these peak water levels whilst the maximum amplitude was the maximum of these. This analysis process was carried out for each wave gauge across the entire range of frequencies tested at both 0.01m and 0.02m amplitudes. Both the average and maximum amplitudes are shown within Figure **5.3** and Figure **5.4**, as well as within Appendix B, to allow comparison to the amplitudes induced by the wave paddles and to those predicted to have occurred using the shoaling coefficient at each of the four wave gauges.

4.2 Qualisys Sensor Data

Following the analysis performed on the raw wave gauge data the nature of the investigation merited detailed analysis be conducted for the data obtained through the Qualisys sensors. This section of the report details the methods used to establish the maximum and average amplitude of the sensors movements and hence of the

pontoon at that point. In addition, the average range of movement of each sensor was calculated; this was not necessarily the same as the amplitude. Another set of analyses was conducted and the average gradient and maximum gradient reached by the pontoon throughout each wave run was calculated.

To ensure consistency and to allow like for like data comparisons, the Qualisys sensors recorded data with a sampling rate of 128Hz. It should be noted, however, that the Qualisys data is precise to the nearest thousandth of a millimetre. This means the largest possible error within the results is 500 nanometres, it was recognised this potential error characteristic is a magnitude of 100 greater than that within the wave gauge data. The accuracy of this data is to be discussed within Section 6.2.

Due to the nature of the modular pontoon and the uniform bathymetry of the coastal basin the results of each pair of sensors (1 and 2, 3 and 4 etc.) will be very similar and as such is spilt into two separate data series for clarity. Throughout the remainder of this report sensor series 1 will refer to sensors 1,3,5,7 and 9. Similarly sensor series 2 will refer to 2,4,6,8 and 10.

4.2.1 Maximum and Average Amplitudes

The maximum and average amplitudes for the data attained through the Qualisys sensors was analysed using Matlab in the same way as the amplitudes from the wave gauges, hence the method of analysis will not be laboured upon at this point. Results from this analysis can be located in Appendix C.

4.2.2 Average Range of Movement

In order to calculate the average range of movement of the pontoon as a result of the waves, a Fast Fourier Transform (FFT) was conducted upon the recorded data. This was done to convert the data from the time domain to the frequency domain. The FFT was performed between the same time increments used for the maximum and average amplitudes for consistency. This FFT output is in the form of complex numbers which can then be used to provide information on the amplitude of the pontoon. By plotting the absolute values of the complex numbers obtained from the FFT the graphic out output as shown within Figure **4.4** below can be attained. For clarity, the output is only provided up until a frequency of 0.25Hz as following this point the corresponding amplitude is equal to zero. The full output can be found within Appendix D.

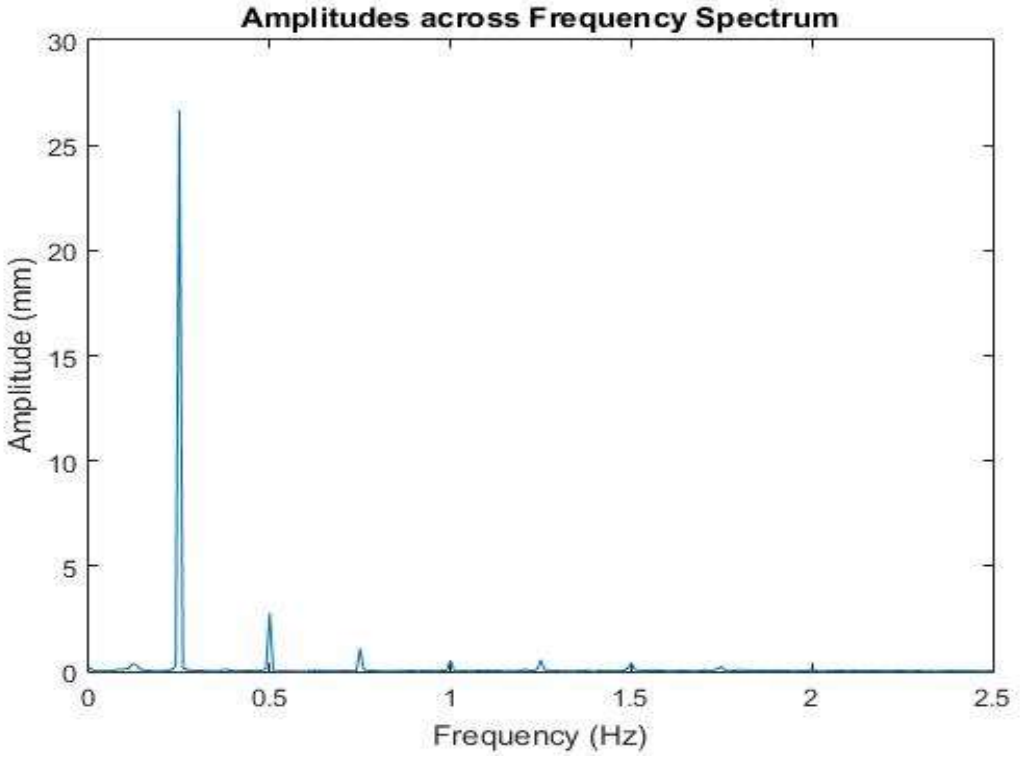

Figure 4.4 - FFT Output – Reduced Axis - 0.25Hz – Sensor 1

Figure **4.4** describes the various components of the wave motion experienced at the Qualisys sensors. The data shown represents Qualisys sensor 1 during the wave run where the amplitude was equal to 0.01m and frequency equal to 0.25Hz. The maximum peak represents the wave function created using the wave paddles, whilst the smaller peaks are presumed to be the result of wave reflections and abnormalities induced by wave breaking effects. There is a large peak at 0.25Hz; this corresponds to the frequency of the induced wave. The magnitude of this peak can be said to be the half of the average range of movement. This is different from the amplitude as the wave motion seems to be weighted towards peaks rather than troughs. The results were then doubled to get a value for the full range of movement for each sensor.

4.2.3 Gradient Calculation

The final piece of analysis which was conducted was that of establishing the gradient the pontoon reached during each wave run. Both the average gradient of the pontoon and the maximum gradient of the pontoon were calculated. These were both established using a straightforward method. If the experimental run to be analysed was that with amplitude of 0.01m and a frequency of 0.25Hz the following would have been conducted. Firstly, the Qualisys data had to be separated dependant on sensor number. As given the nature of the grid of sensors, the pontoon surface along its length was described by the levels at sensors series 1 and at sensor series 2 independently. Based on the surface levels at these points for a given time instance, the level of the remainder of the pontoon was interpolated. The effect of this is demonstrated on Figure **4.5**, this shows the pontoon level at a point where time is equal to 60 seconds for both series.

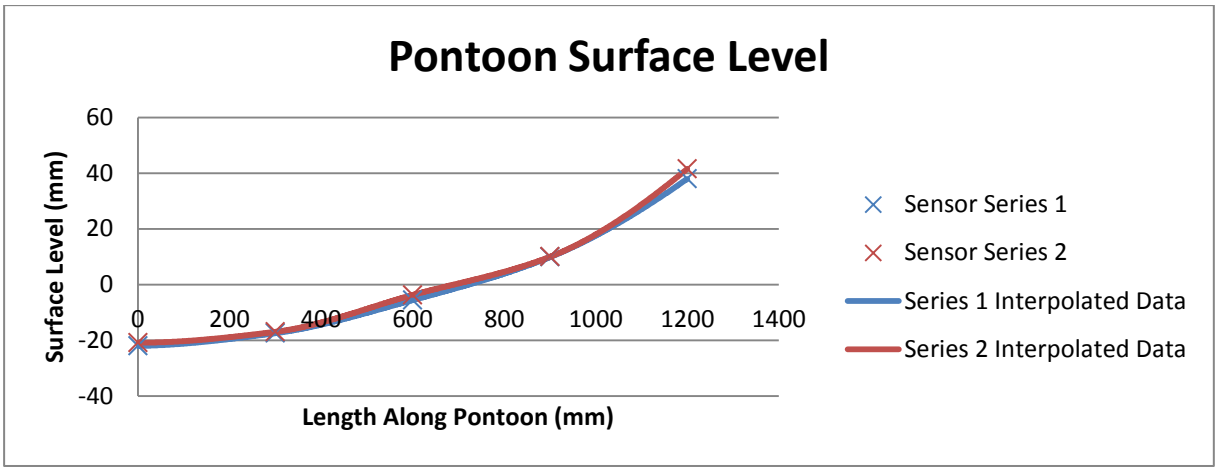

Figure 4.5 - Surface Level of Pontoon at time 60 seconds into wave run

From this information, the gradient of the pontoon surface at each point was calculated. This was repeated for every time instance throughout the experimental run. This resulted in a list of gradients detailing the gradient at each point along the pontoon for every time instance throughout a run. The maximum gradient reached and the average gradient could then be obtained from this data. For example, the maximum gradient reached by the pontoon for the 0.25Hz with 0.01m amplitude run was 0.15; this is equivalent to a 1 in 6.71m slope. For the same run, the average gradient reached was 0.03; equivalent to a 1 in 34.66m slope. Using the same process the maximum and average gradients were calculated for all other frequency wave conditions for amplitudes of both 0.01m and 0.02m waves. The maximum gradients and average gradients across the course of the experiments are shown in Figure **4.6** and Figure **4.7** respectively.

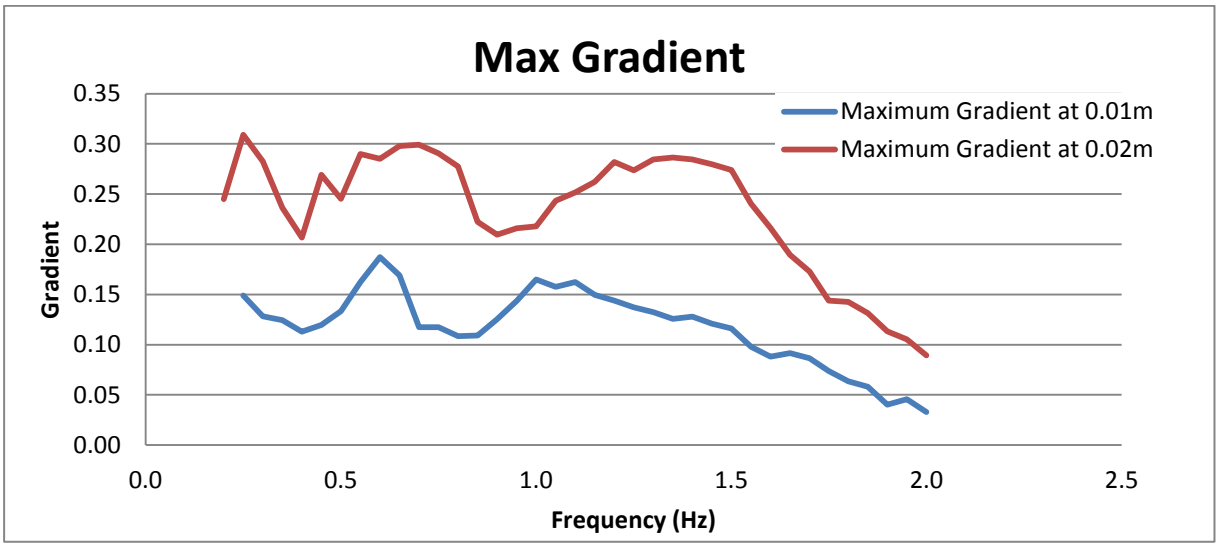

Figure 4.6 - Maximum Gradient reached by Pontoon across experiments

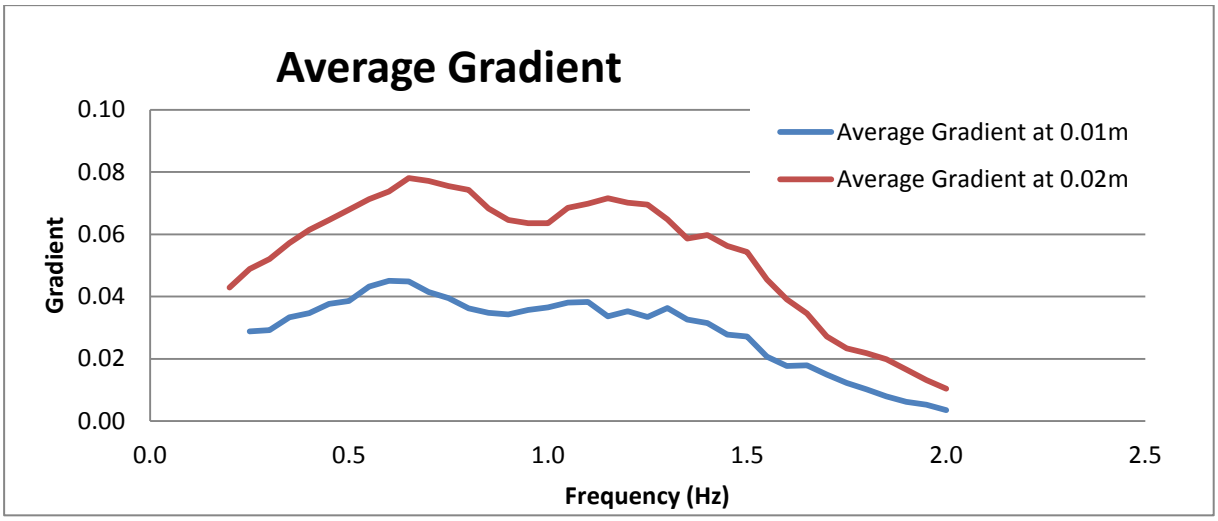

Figure 4.7 - Average Gradient reached by Pontoon across experiments

5 Results

This section details the final output resulting from the completed data analyses. Data presentation within this section may not be fully complete due to the significant volumes of data collated. As such data presented may have been truncated to illustrate a specific point or conclusion. Full information data tables and more detailed graphical plots can be found in the appendices.

5.1 Wave Gauge Data

The plots below detail the average amplitudes and the maximum amplitudes recorded throughout the experiment. Additionally, each figure also demonstrates the amplitude predicted to occur using the shoaling coefficient. Finally, the amplitude induced by the wave paddles is also plotted to allow easy comparison. To avoid an overloading of figures only those relevant to wave gauge 1 are included. All other plots can be found within Appendix B.

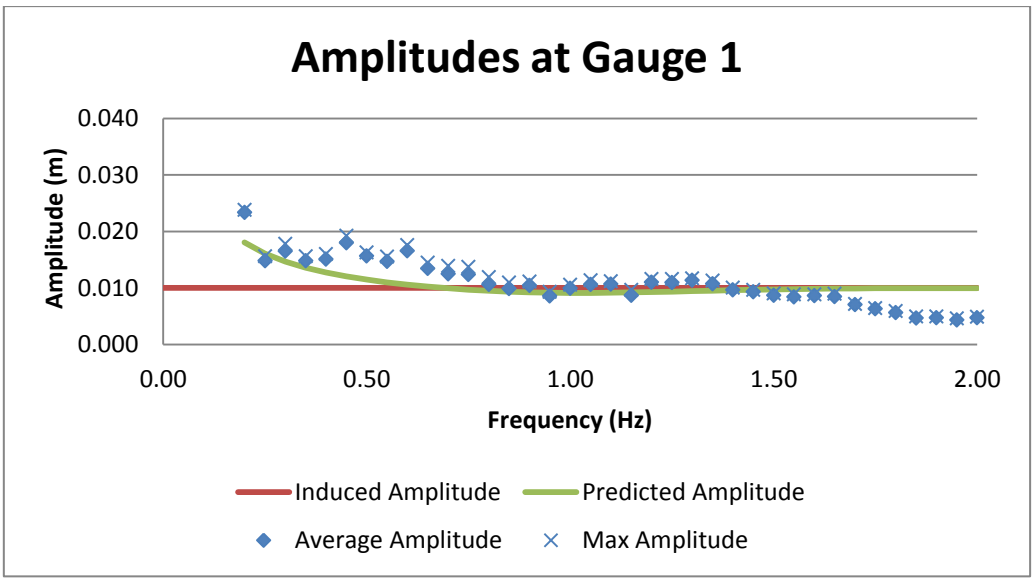

Figure 5.1 - Amplitudes at Gauge 1 under 0.01m wave amplitude conditions

As can be seen in Figure **5.1** across the full range of data there is very little discrepancy between the maximum amplitude and the average amplitude of the waves experienced across wave gauge 1. It is clear, however, that shoaling has a definitive effect upon the amplitude of the waves. At lower frequency waves the exhibited wave amplitudes are almost without fail greater than those predicted based on the shoaling coefficient. At higher frequencies, the experienced wave amplitudes fall below both the induced and predicted amplitudes. It is believed that this is due to the effect of wave reflection from the back of the coastal basin or due to the breaking of waves further offshore than the wave gauge.

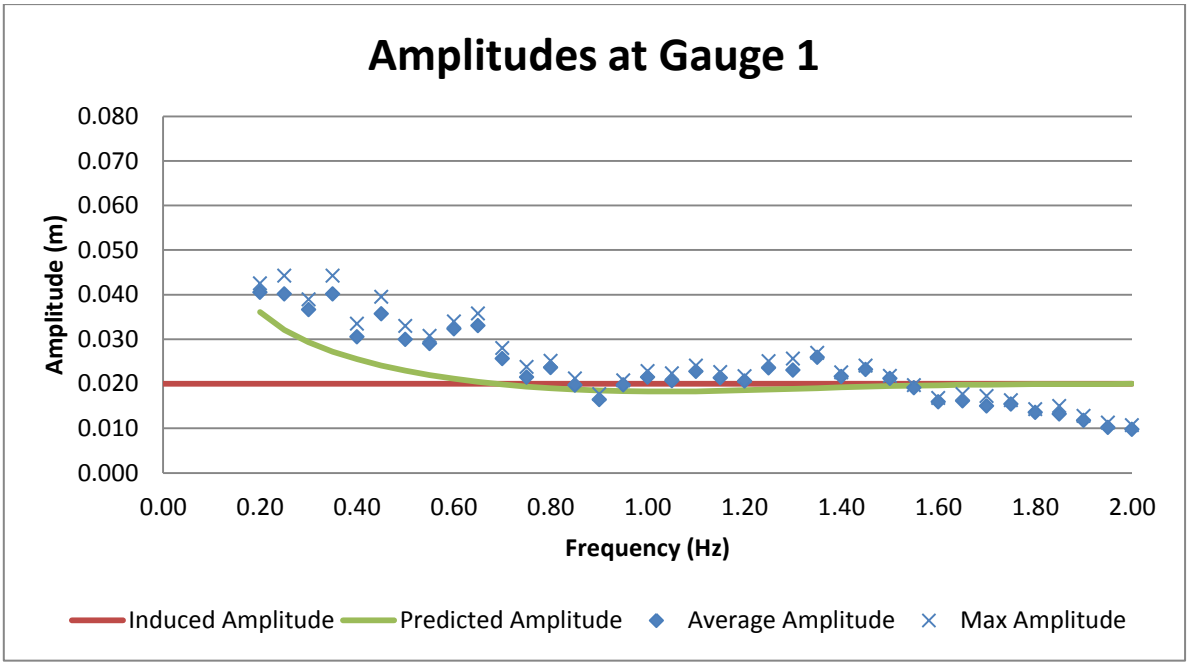

Figure 5.2 - Amplitudes at Gauge 1 under 0.02m wave amplitude conditions

Figure **5.2** demonstrates the equivalent information but for waves of amplitude of 0.02m. As can be seen the same trend is followed as the 0.01m waves. In low frequency waves the measured amplitudes were greater than predicted, whilst at high frequencies the predicted amplitude provided an over estimate. It can also be observed that the discrepancy between the average amplitude and the maximum amplitude is greater when operating at low frequencies.

Based on these data sets and the similarity between both figures it is reasonable to conclude that the predicted amplitude is most accurate between 0.75Hz and 1.5Hz, however it is still not a perfect fit. Either parameters not included within the method of prediction are affecting the results, or the waves modelled did not match the input wave characteristics.

An additional relationship which can be seen, albeit indirectly, is that in terms of magnitude the amplitudes output for the 0.02m amplitude wave is approximately double that of the 0.01m amplitude wave. The data supports this finding across the plots for the remaining three wave gauges.

5.2 Qualisys Data

The data obtained from the Qualisys, following analysis, resulted in various plots which help describe the motion of the model modular pontoon due to the waves induced.

The first data point, where frequency is 0.2Hz, appears to be anomalous for the 0.01m amplitude wave conditions. This is suspected to be due to human error or data corruption when saving the data files of the Qualisys data results. As such this data point has been excluded from all figures and calculations.

5.2.1 Maximum and Average Amplitudes

Figure **5.3** shows the maximum and average amplitudes which were calculated across the range in frequencies as measured from sensor 1.

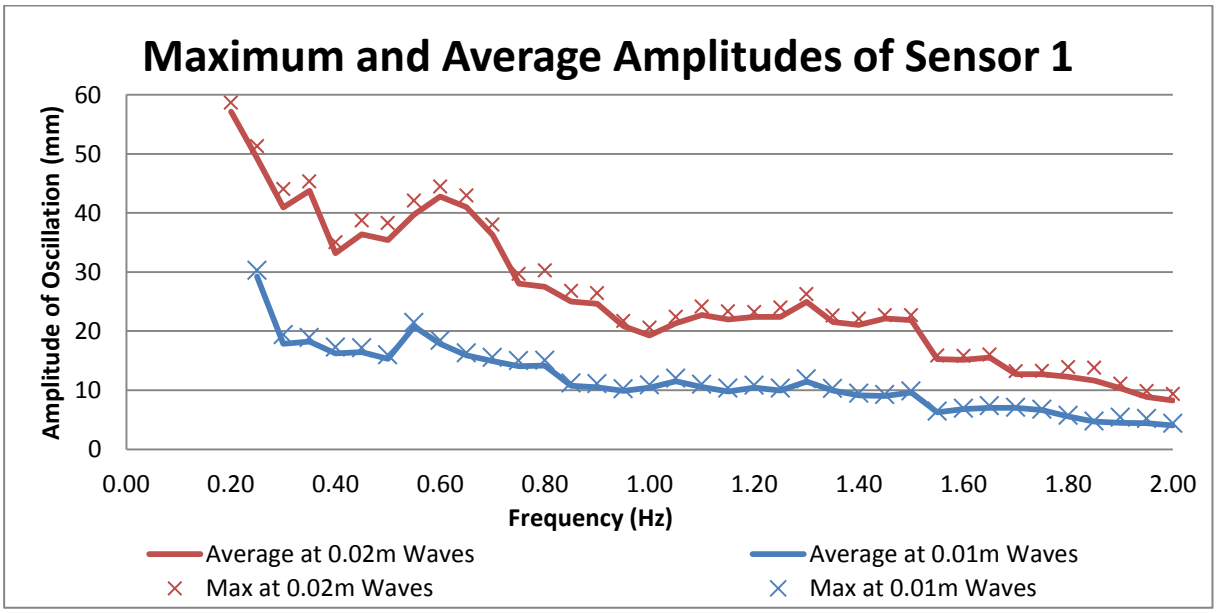

Figure 5.3 - Maximum and Average Amplitudes at Sensor 1

As can be seen in the figure, a similar relationship is shown to that demonstrated by the wave gauges. At low frequencies, the amplitudes of oscillation, both maximum and average, are greater. These amplitudes then decrease as the frequency is raised, the difference between the amplitudes of the 0.02m amplitude waves and the 0.01m amplitude waves is also decreased and the frequency is raised. There is an unexpected peak in both data sets at around 0.65Hz, which does not follow the trend; this is considered as being possible due to wave breaking, or perhaps resonance is taking place.

As sensor 1 is towards the offshore end of the pontoon, the same information obtained from sensor 9, towards the landside end of the pontoon, is displayed on Figure **5.4** for comparative purposes.

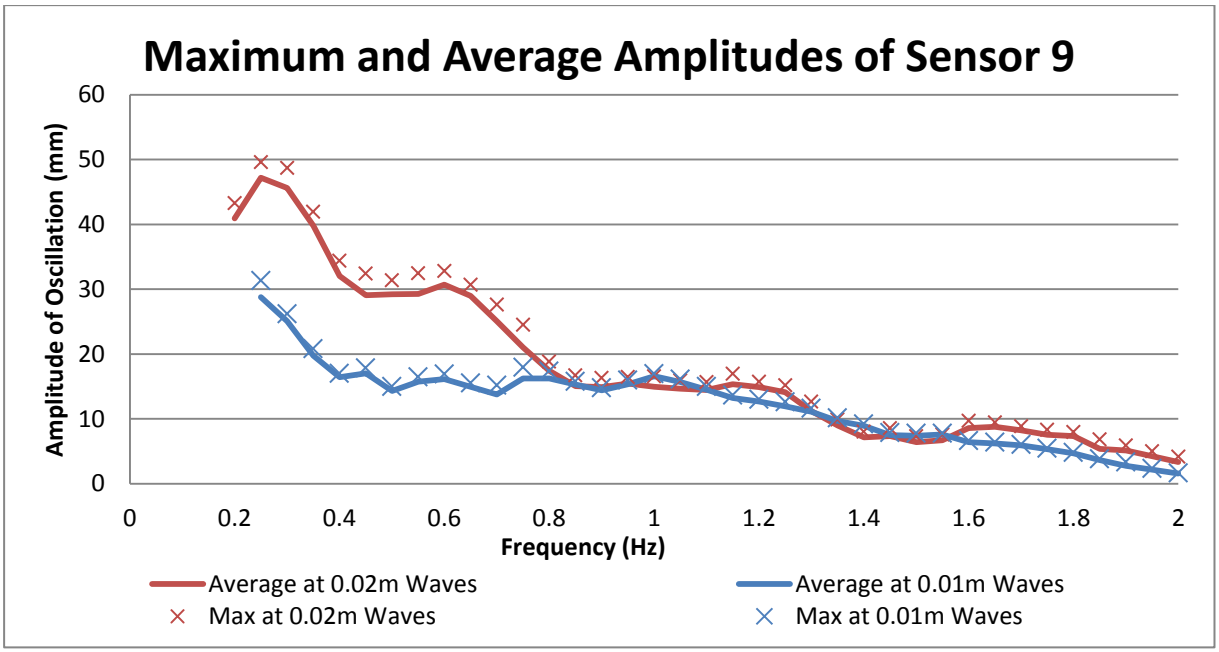

Figure 5.4 - Maximum and Average Amplitudes at Sensor 9

As can been seen in the figure the same relationships are followed. This time however, for the 0.02m amplitude waves, the values resulting from a frequency of 0.2Hz are lower than would be expected. It is also critical to note that the variation between the two sets of results is significantly reduced at this sensor. Once the average amplitudes reach the same level at around 0.8Hz they remain similar for the duration of the frequency ranges.

5.2.2 Average Range of Movement

The average range of movement as output through the data analysis is demonstrated graphically in Figure **5.5** to show the movement occurring at sensor 1. As would be expected this is similar to that of the average and maximum amplitudes. The values tend to be larger however by 15 – 20 mm across the data sets.

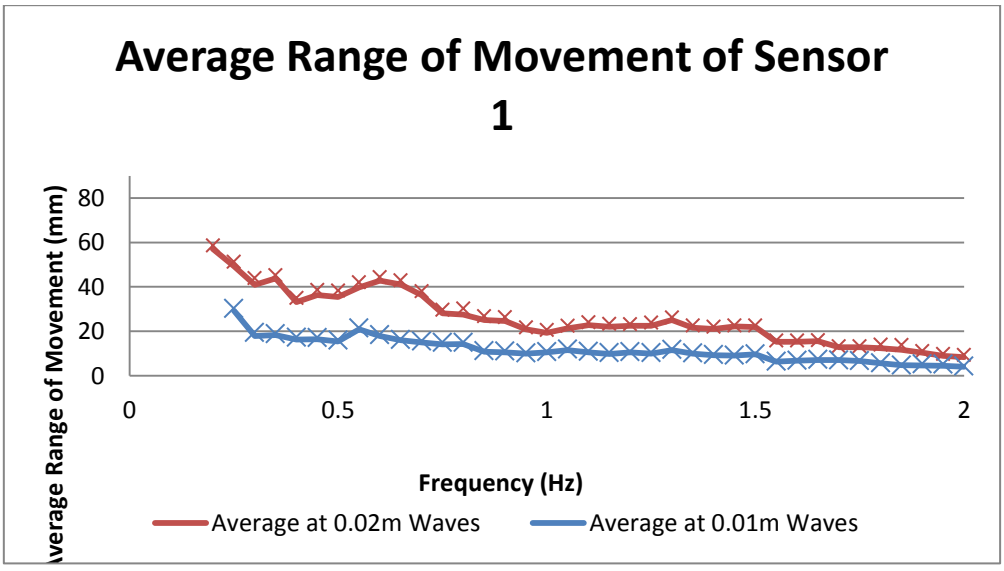

Figure 5.5 - Average Range of Movement at Sensor 1

The remainder of the sensors can be found shown in a similar manner within Appendix E, which shows the average range of movement for each frequency test across both amplitudes.

5.2.3 Pontoon Gradient

The information regarding the pontoon surface gradient is plotted previously; Figure **5.6** and Figure **5.7** demonstrate this information in terms of the slope of the pontoon surface rather than in terms of the gradient.

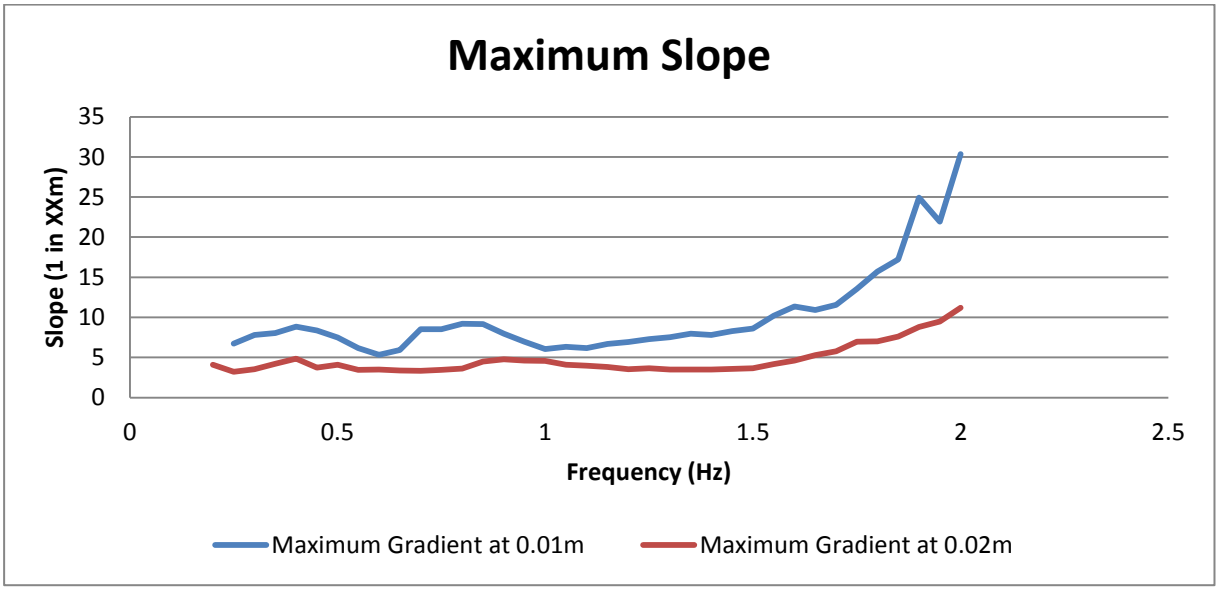

Figure 5.6 - Maximum Slope achieved by Pontoon Surface

It is evident from the information as presented that the pontoon reaches a much steeper maximum slope generally when subject to waves with amplitude of 0.02m. The slope for the 0.02m amplitude waves remains fairly constant at around a 1 in 4m slope across most frequency values up until around 1.5Hz where the slope becomes more gradual. The maximum slope for the waves with amplitude 0.01m is similar in nature however it remains much less constant across the breadth of the experiment; although the slope is more gradual, it seems to be more vulnerable to variance due to frequency. Another difference between the two data sets is that the slope begins to become more gradual at a lower frequency than that of the 0.02m amplitude waves. The exact frequency at which the slope starts to become more gradual is hard to determine due to its variance, but is approximately 1.25Hz.

In addition the informational data regarding the average gradients across the pontoons surface can also be represented in terms of an average slope. This allows easier comprehension when observing the data. Figure **5.7** demonstrates this information.

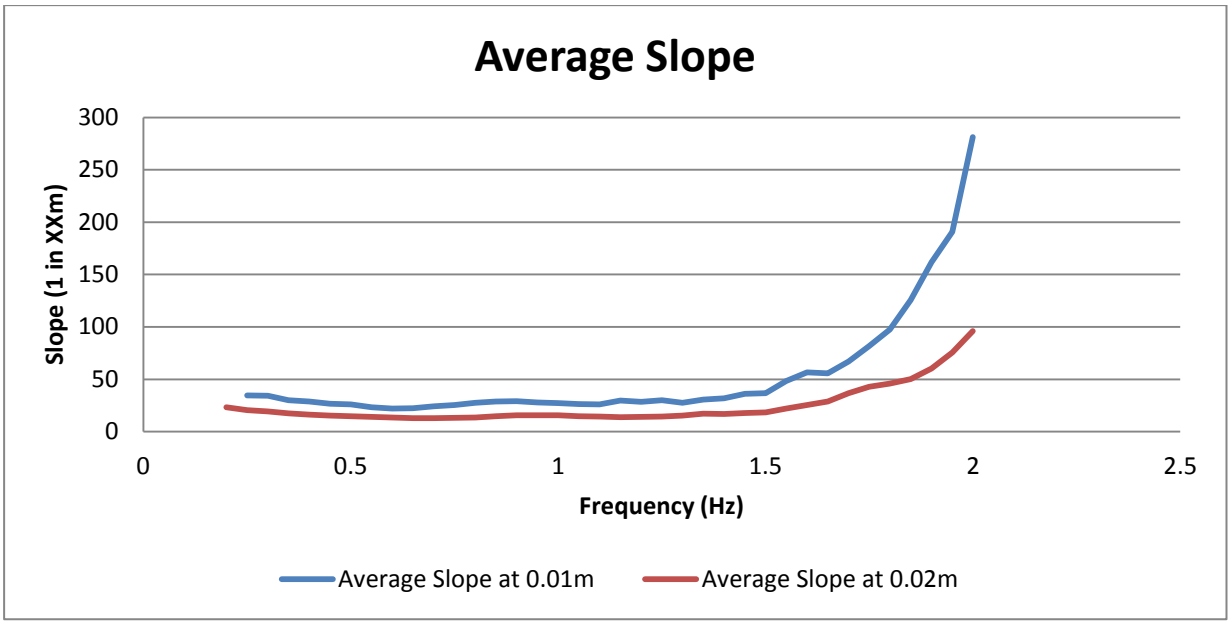

Figure 5.7 - Average Slope achieved by Pontoon Surface

From this, the average gradient is significantly less than that of the maximum gradient reached. The average slope at 0.02m amplitude waves remains constant at around 1 in 15m, compared to the maximum of around a 1 in 4m slope. Additionally, the slope reached under 0.01m amplitude conditions seems to be much more consistent across lower frequency ranges and then becomes much more gradual around 1.5Hz. When the modular pontoon is subjected to waves of frequency greater than 1.75Hz the slope is so gradual it may as well be considered flat for all intents and purposes.

Looking at the equivalent figures for the data in terms of gradients is more helpful at this point as the numerical variance across results is more easily shown. Although the gradient within the lower frequencies is relatively consistent, the gradient data shown a definitive peak at roughly 0.6Hz across each both the average and maximum gradient data sets.

5.3 Repeats

The data given before could be determined to be useless if it is established that the results and data extracted from this was concluded to not be replicable and just a one-off result. For that reason, wave runs for 1.0Hz, 1.5Hz and 2.0Hz for the 0.01m amplitude wave conditions were repeated several times to confirm the repeatability of the pontoon response observed. This section details the output of these repeats.

5.3.1 Maximum and Average Wave Amplitudes

Calculations were conducted based upon the data obtained from the wave gauges for the repeated wave runs. What follows are several tables which describe the output of the calculations and analyses listed previously. For simplicity, only the information relevant to the repeat of the wave with frequency 1.0Hz is included within this section within Table **5.1** and Table **5.2**. Pertinent information regarding other wave runs can be found in Appendix F.

Table 5.1 - Average Amplitude for 1.0Hz frequency wave

Wave Run	Average Amplitude at 1.0Hz (mm)			
	Gauge 1	Gauge 2	Gauge 3	Gauge 4
1	9.949	8.417	9.232	9.406
2	10.225	9.237	9.318	9.199
3	10.126	8.099	8.887	9.301

Table 5.2 - Maximum Amplitude for 1.0Hz frequency wave

Wave Run	Maximum Amplitude at 1.0Hz (mm)			
	Gauge 1	Gauge 2	Gauge 3	Gauge 4
1	10.560	9.151	10.224	10.517
2	10.665	10.187	10.438	10.232
3	10.731	8.563	9.702	10.232

It can be seen from the information in these tables that the results from the analyses on these repeated data sets are very similar. The most significant difference evident between the different wave runs is that between the calculated amplitudes of wave run 1 and 2. Here there is a maximum difference of 0.8mm and 1.0mm for the average amplitude and the maximum amplitude respectively.

5.3.2 Amplitudes and Average Range of Motion of Pontoon Surface Level

Once again only the results of the various analyses conducted upon the data for the 1.0Hz wave condition will be given in this section. This information is shown in Table **5.3** and

Table **5.4**; relevant information for the 1.5Hz and 2,0Hz wave conditions can be found in Appendix F.

Table 5.3 - Average and Maximum Amplitude of Pontoon for wave frequency of 1.0Hz

Sensor No.	Average Amplitude for Wave Run at 1.0Hz (mm)			Maximum Amplitude for Wave Run at 1.0Hz (mm)		
	1	2	3	1	2	3
1	10.446	10.900	10.268	10.172	9.957	9.846
2	9.900	10.297	10.030	9.710	9.516	9.433
3	10.488	10.873	10.110	10.012	9.610	9.550
4	9.906	10.288	9.866	9.786	9.384	9.352
5	11.049	11.427	11.713	11.469	11.258	10.892
6	10.960	11.571	11.480	11.374	11.059	10.934
7	14.891	15.581	14.931	14.681	14.428	13.998
8	14.976	15.370	14.719	14.349	14.136	14.033
9	16.581	16.940	16.047	15.703	15.661	15.440

10	15.624	16.039	15.360	15.383	14.917	15.074

Table 5.4 - Average Range of Motion of Pontoon for wave frequency of 1.0Hz

Sensor No.	Average Range for Wave Run at 1.0Hz (mm)		
	1	2	3
1	19.917	19.327	19.001
2	18.821	18.564	18.438
3	19.262	18.404	18.025
4	18.386	17.773	17.408
5	19.370	19.360	18.797
6	19.023	19.177	18.801
7	23.700	22.787	22.474
8	23.313	22.286	21.984
9	25.722	24.507	23.918
10	25.531	24.720	24.796

The results obtained and presented in the tables above provide confidence as to the replicability of the behaviour of the modular pontoon; the results seem to be repeatable across the extent of the study. The second and third wave run are drastically more like each other than they are to the first wave run. For the 1.0Hz frequency wave the initial wave run results in higher values for both maximum and average amplitude as well as the average movement. The 1.5Hz frequency waves show an oddity at sensors 4 and 5, where the output values are much higher during the initial run that the following repeats, this is explored in Section 6.2.4.

There is a large difference between the maximum amplitude and average amplitude of the data at sensor 7, interestingly the difference at the corresponding sensor (sensor 8), is similar to the rest of the data sensor array. The cause of this is not known and based upon correlation without other readings is assumed to be due to some form of interference.

5.3.3 Pontoon Surface Gradient and Slope

From Table **5.5**, the gradient shows relative consistence in terms of the average when compared with the slight variance in the maximum gradient. Much like the rest of the data from repeats the primary wave run output a higher value that the following two wave runs.

Table 5.5 - Maximum and Average Gradient and Slope at 1.0Hz

Wave Run	1.0Hz Frequency			
	Average Gradient	Average Slope	Maximum Gradient	Maximum Slope
1	0.0365	27.38	0.16494	6.06270
2	0.0356	28.11	0.15311	6.53143
3	0.0352	28.40	0.14930	6.69798

6 Discussion

6.1 Wave Gauge Data

Within the data output from the maximum and average values for amplitude at the wave gauges there is a relatively sizeable discrepancy between the predicted values and those which occurred. The most likely reason for the difference is the reductionist method of calculation used to work out these predicted wave amplitudes. The first approximation which is made for the method to be valid is that there is no loss or gain of energy from the system. However, this means that factors such as that of friction between the wave and the sea bed are ignored. In respect of the coastal basin, friction with the sides of the basin is also a consideration. The effect of this friction would have decreased the embodied energy of the wave and resulted in smaller wave heights and therefore smaller amplitudes. This effect would occur across the range of results and lead to the predicted values being an over estimation. As this is not a problem with the set of data it can be assumed that the effect of friction is not severe enough to be significant. To gain more accurate predicted values for the wave amplitude due to shoaling, the shoaling coefficient could be refined to increase the reliability of the value. LeMehaute and Webb (1964) computed a refined version shoaling coefficient using third order Stoke's equations rather than linear wave theory. Their study showed a larger shoaling coefficient than that based on linear theory; this would result in larger predicted wave heights if applied to the current study. These wave heights would be more similar to the low frequency wave amplitudes which were measured, however this would not fit the data resulting for high frequency waves. With more confidence that the wave height prediction was accurate, using the depth at each Qualisys sensor the amplitude at this point could be directly calculated. This would allow direct comparison between the amplitude of the pontoons movement and that of the wave beneath it, rather than using the amplitude at a point adjacent to the pontoon as was the approach for this study.

Although the wave gauge data was recorded to a high degree of precision there is no guarantee as to the accuracy of this data. It is assumed that the data is accurate for all analysis detailed within the report although it is import to note that this is not the case, for example distortion caused by surface tension around the sensor itself may occur. To assume the data is entirely accurate would be a gross oversimplification.

6.2 Qualisys Data

For all results, which were gained from the Qualisys data there appears to be an anomalous point for the 0.01m amplitude data series. The data point in question is the 0.2Hz frequency point. As this error seems to be present across the entire set of recorded data it is assumed that the cause is data corruption or human error during the modelling phase of the experiment. It is possible that a file name may have been overwritten during data storage. From the results obtained through analysis upon this anomalous data set, it is believed that data for a 2.0Hz wave was saved in place of data for the 0.2Hz wave. This data point has been ignored when drawing any conclusions as to trends and patterns shown by the data and has been removed from any relevant figures. As such any and all errors that may have been introduced by this anomalous data set have been mitigated.

Much like the wave gauge data the Qualisys data was recorded to a high degree of precision. The accuracy of the data can be interpreted somewhat based upon the calibration of the Qualisys cameras. An issue is, however, that is the calibration procedure is not conducted effectively then the results for an entire days testing can be less accurate as a result.

6.2.1 Fast Fourier Transform Results

The FFT which was used as part of the method for several aspects of the analysis yields an output which gives a useful perspective into the movement of the modular pontoon. Figure **6.1** shows the output of the FFT for waves of a frequency of 0.6Hz where for clarity only data up to 10Hz is shown, as the amplitude beyond this point is equal to zero. This is plotted for the movement at Qualisys sensor 10, as being the closest to the shore was most likely to have experienced wave reflection and less likely to be biased from the effects of wave breaking.

From Figure **6.1**, aside from the peak at 0.6Hz representing the frequency of the induced wave there are many other peaks of significant height. This means that aside from the amplitude reached due to the 0.6Hz frequency the pontoon was also reacting at various other frequencies. From close analysis of the data it can be observed that these peaks were all multiples of the input frequency. To put this is physical terms the modular pontoon was reacting to the waves being reflected from the fixed sea wall in addition to the original wave. As discussed within Section 2.2 these reflected waves would have reduced amplitude when compared to the original, hence the diminishing amplitude of each reflected wave shown within the graphical data. These reflected waves would interact within the incoming waves and have a distorting or dampening effect across the remainder of the wave gauges.

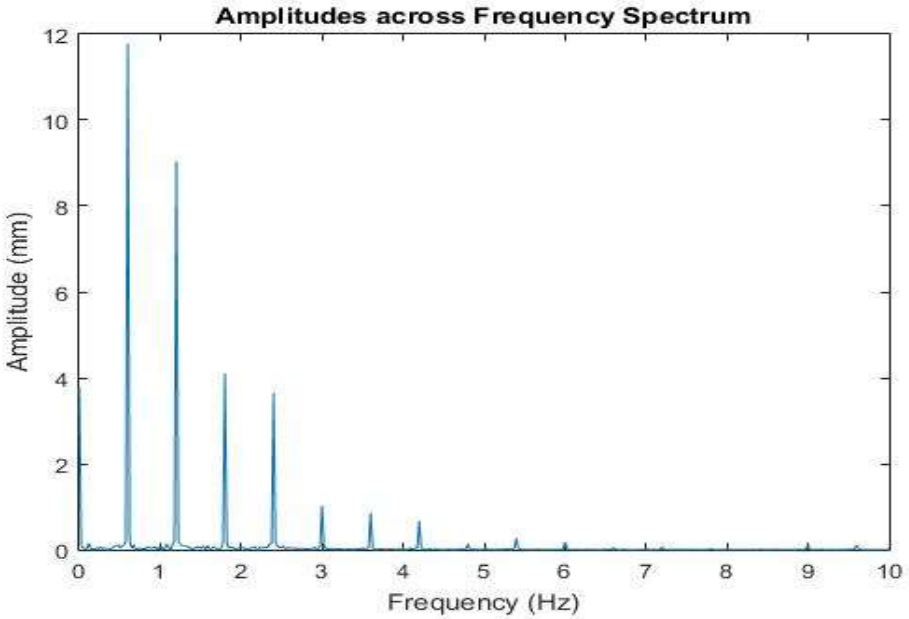

Figure 6.1 - FFT Output - Reduced Axis – 0.6Hz – Sensor 10

6.2.2 Average and Maximum Amplitudes

Looking at the plots of maximum and average amplitudes of the pontoons movement at each of the sensors there are several patterns and behaviours which are identifiable. At the first pair of sensors, 1 and 2, there is a distinct peak across all

experimental data at around 0.65Hz. Although it is possible that these peaks are due to waves breaking at the sensor location for these frequencies, it is deemed that this is unlikely as these sensors are the furthest offshore and should not fall within the breaking zone.

This effect is more likely induced by some unusual movement of the pontoon itself. This movement could be a sign of resonance with a frequency around this area; alternatively, it could be a result of the model being unable to move correctly in accordance with waves of this frequency. These hypotheses could be established but would require further testing within this frequency range. From observing the remaining pairs of sensors a similar peak is present at sensors 5 and 6 at a frequency of 0.5Hz, interestingly this peak however is only present for the 0.02m amplitude waves. The idea that this peak develops only with certain wave amplitudes leads to suggest that the peak for these sensors is a result of the wave breaking at or near the sensors.

The same theory could explain the peak located in the result for sensors 7 and 8, where there is a clear peak around 0.75Hz. However, this peak is also present in the data for the 0.01m amplitude waves, albeit at a frequency closer to 0.6Hz. As these sensors are now certainly within the breaking zone it is expected that both these peaks are due entirely to the presence of breaking weaves directly beneath the pontoon at the sensors location, again this cannot be confirmed without further testing.

6.2.3 Average Range of Movement

The average range of movement was also calculated as part of the report. As noted during Section 5.2.2 these values tend to be larger by 15-20mm than the maximum and average amplitudes as calculated previously. This is expected to be because the maximum and average amplitudes have a centre of oscillation which is not necessarily the still water level; the calculations however operate based on the assumption that this is the case. Being taken from the average peak height, the range of movement statistic can be calculated independent of the still water level and hence may be a more accurate representation of the pontoons movement. The peaks within amplitude values previously mentioned are not as prominent within the average range of movement values; this may suggest that they were at least partially present due to the method of calculation. The exception to this is the peak located at 0.02m amplitude and 0.75Hz frequency for both sensors 7 and 8. These peaks are, if anything, more pronounced than those demonstrated within the results gained in terms of amplitudes. This reinforces the idea that the peak at this point (and respectively at 0.6Hz for 0.01m amplitude) is due to the effect of wave breaking at the location of the sensor. It should be noted that the effect of the wave breaking cannot be isolated completely as it may also be partially the effect of the low frequency of the induced wave.

In a real-world situation, sudden heave due to the passing of a breaking wave beneath the pontoon would be disadvantageous to the condition of any objects on the pontoons surface and could pose a danger to property or people. Certainly, the viability of a modular pontoon for use as a beach landing or small pier may be called into question when operating within the breaking zone, particularly when experiencing waves with relatively low frequencies.

Another interesting point to be aware of is within the figures detailing the average range of movement of sensors 9 and 10. Unlike other sensor information these average movements values are very similar throughout the full range of tested frequencies. It is thought that there are two possible reasons that could be responsible for this outcome. The first of which is that this sensor was present closer to the shore than the waves were breaking, this would have the effect of rendering the difference in amplitude between the two wave conditions null and void, and thus would explain the very similar movement values. The other reason is that the model pontoon may have become partially grounded at the land side end during these experimental runs, this would mean that although the pontoon would be able to float over the peaks of the waves reaching the shore, it would not be able to fill any troughs which would be present at the other sensor location due to the proximity of the bed level limiting this range of movement. It is thought that the similar values occurring at sensors 9 and 10, as demonstrated within Appendix E, is due to a combination of these factors.

6.2.4 Average and Maximum Slope of Pontoon Surface

When looking at the results of the gradient and slope calculations it is relatively easy to get an idea into the behaviour of the modular pontoon. The maximum values for the pontoon slope obviously show a significantly steeper slope than those of the average values; however, they also seem to show more variance. This is likely due to the nature of the wave beings simulated by the coastal basin. As the waves being produced are regular and sinusoidal it is expected that average values will be as a heavily influenced by the continued and repetitive wave motion. If the motion of the pontoon was perfectly sinusoidal the resulting average gradient would be zero. As such the output, average gradient is simply a measure of what the average gradient could be expected to be at any particular time. Emphasis should not be put upon these resulting average amplitudes as they are more of an indicator than a useable value.

The maximum slopes are attributed to one of the following phenomenon. The first of which is wave set up, as the gradient calculations were performed across the full range of data this means they have the potential to include gradients reached in the early stages of each wave run where the sea state of the coastal basin is still building up. It is equally possible that the larger gradient is a result of an irregular movement of the model pontoon; during some wave runs the model was observed to get caught upon the simulated fixed sea wall. This could give the impression of a higher gradient than what was experienced if it caused a sensor to be raised further than where it would have been due to wave action.

Of course, all gradient and slopes calculated rely on the method of interpolating the pontoon surface level between the recorded sensor levels. If the method of interpolation used does not accurately represent the actual pontoon surface level, then these slopes cannot be relied upon too heavily. As such these slopes are used as an indicator of those reached during the actual experiment rather than as definitive results. If the experiment were to be repeated it would be conducted using a greater number of sensors to gain a better understanding of the vertical deformation across the length of the pontoon.

An interesting effect across all the slope data is that the wave frequency has a lesser effect upon the slope of the pontoon surface elevation until a higher frequency is

reached. That is not to say that there is no effect, the gradient is higher when the frequency is around 0.6Hz. This corresponds to the peak in amplitude identified previously at this frequency range for sensors 0 and 1. It is felt that this reinforces the belief that there may be some resonance effect occurring around this frequency range. This could be explored further through additional wave modelling and testing, possibly with the conduction of a nested parametric study investigating the range of frequency to ensure the observed peak in data was a genuine occurrence.

6.3 Scale and Model Effects

It is important to note that the model used for this experiment was by no means an accurate representation of a real-world pontoon. As such care must be taken when generalising any conclusions drawn from this experiment to real world applications. Although it was attempted to reduce errors through the design of the model it is anticipated that the scaled model in question suffered from several scale and model effects. Each of these may have produced error and inaccuracy into the results.

Scale effects which will have influenced the results taken from this study are those of sea bed friction, viscosity and surface tension. This is a result of incongruence between the Buckingham π parameters associated with the model and the real-world pontoon. Due to the nature of scaling during this study scaling was based entirely upon calculated wave heights and the generation capabilities of the coastal basin. As such it is not known if any of these parameters are maintained between the model and real world pontoon. Each of these factors has the potential to significantly affect the result, especially if a combination of them independently affects the result.

The sea bed friction in a real-world situation effects the propagation of a wave, albeit not majorly. The coastal basin has a smooth base hence this friction factor is assumed to be negligible in comparison to the roughness of a sandy sea bed with plant life and debris. The result of this differential in sea bed roughness is that waves may break later through the experiment than they would in a full-scale situation. This has a significant effect on the results and the breaking of waves is responsible for many of the eccentricities across the data due to the higher wave heights immediately before breaking. The effect of viscosity and surface tension although present, are thought to be less significant in this case have not been fully explored.

Several model effects were also noted to be present though the experiment. These have the potential to be just as damaging to the validity of the results as the scale effects previously mentioned. The first model effect, and possibly the most significant, is the inability of the model to accurately model the bending between modules which is present in the full-size pontoon. By using a fabric connection, the model modular pontoon is too flexible, as such it may cope with some waves better than the full-size pontoon would be likely to. Relating to this is the second model effect, that of the buoyancy of the modular pontoon. As the finalised model is more buoyant that the full-size version it has to be questioned whether the model responds to the induced waves in the same manner as a full-size pontoon would react. If the model pontoon responds to a manner too dissimilar then perhaps it is not realistic to generalise its behaviour to a full-size version. Additionally, although a minor point, the model pontoon was tested in fresh water with a density of 1000kg/m^3, whilst in its role as a pontoon pier structure the seawater would have a density of 1025kg/m^3. This would affect the floating of the pontoon and hence its free board. The effect of this is assumed to be negligible however.

6.4 Repeated Wave Runs

As part of the experimental procedure several of the characteristic waves which were simulated and used to test the modular pontoon were repeated. The aim of this was to confirm the replicability of the results. The outcome of this was confirmation that, in general, the results gained throughout the experiment seem to be possible to replicate to a relatively accurate standard.

For 1.0Hz frequency waves the initial wave run resulted in waves with definitively higher amplitude than the following two wave runs. Referring to data for the maximum and average amplitudes for waves with frequency 1.0Hz this statement is not true across the full range of sensors. In fact, the amplitudes output by the data analyses are only marginally greater than the following wave runs at sensors 5 and 6. Coincidentally these sensors were located in the area where wave breaking had been known to occur. It is assumed that despite the apparent differences in the pontoons response across the remainder of its length, when in the breaking zone, it is the waves breaking themselves which determined the motion of the pontoon. The rest of the pontoon may have been more responsive for the latter runs but this could be due to various factors. Perhaps an issue with the model had occurred and the model had looser connections between pontoon modules allowing more movement. Another possibility is that the tie which held the pontoon back to the sea wall had loosened due to wave action; this would have allowed the pontoon a greater range of motion. Alternatively, and perhaps more reasonably, the waves induced were marginally larger than the following two wave runs. This could be due to minor imbalances in the movement of the wave paddles or some similar phenomenon; the wave paddles were recalibrated part way through modelling to resolve a minor system error. This theory is supported by the average amplitude and maximum amplitude calculated for the two repeated wave runs in which at gauge 4, whose depth matches the sensors most closely, the values are larger than the following 2 wave runs. This can be seen within Table 5.1.

When looking at the resulting data showing maximum and average amplitudes based upon repeats of the 1.5Hz frequency wave it can be observed that sensors 4 and 5 differ between the first wave run and following two wave runs by a greater amount than at other sensors. These sensors could also be said to be in a location where wave breaking is taking place, so a similar conclusion could be drawn as to the values for sensors 5 and 6 at 1.0Hz frequency. This is not supported, however, by the resulting information from wave gauges; because of this it is believed another factor must be responsible for this behaviour. This cannot be fully explained without more extensive testing to explore in further detail.

The final set of results gained from the repeating of these wave frequencies was that of gradient and slope information. As before the first wave run caused the pontoon to react more extremely than the subsequent two wave runs. Although the difference is not enough to cause concern, the fact that it has caused discrepancies across all data sets of repeated wave runs means it should merit further investigation.

6.5 Real World Applications

The maximum and average gradients of the modular pontoon were calculated as this study set out to accomplish. To be suitable for common use the pontoon must conform to certain standards. By using standards set out by various organisations it

could be determined if the modular pontoon could be said to be safe for use by the public.

6.5.1 British and Australian Standards

Currently a standard specifying the maximum suitable gradient for a modular pontoon has not been implemented, or at least has not been found through this projects research. The British Standards Institution (2007) gives a value of relevance that the slope of an articulated ramp, such as one that may be on a block pontoon, should be 1 in 12m. This value may be increased to 1 in 10m if in extreme tidal or sea state conditions. Another standard of relevance that was found was that by Australian Standards International (2001) which suggested that a gangway may have a slope not exceeding 1 in 3.5m (or 1 in 8m if access for disabled persons is required). The average slope of the modular pontoon in this study did not exceed the 1 in 12m given by the British Standards; this is shown within Appendix G.

It is assumed that as the pontoon rapidly changes gradient across its use, the maximum gradient reached should therefore be taken as the more critical gradient rather than the average. The maximum gradient is shown in Figure 6.2 to allow this to be easily comparison to the 1 in 3.5m and 1 in 12m slope.

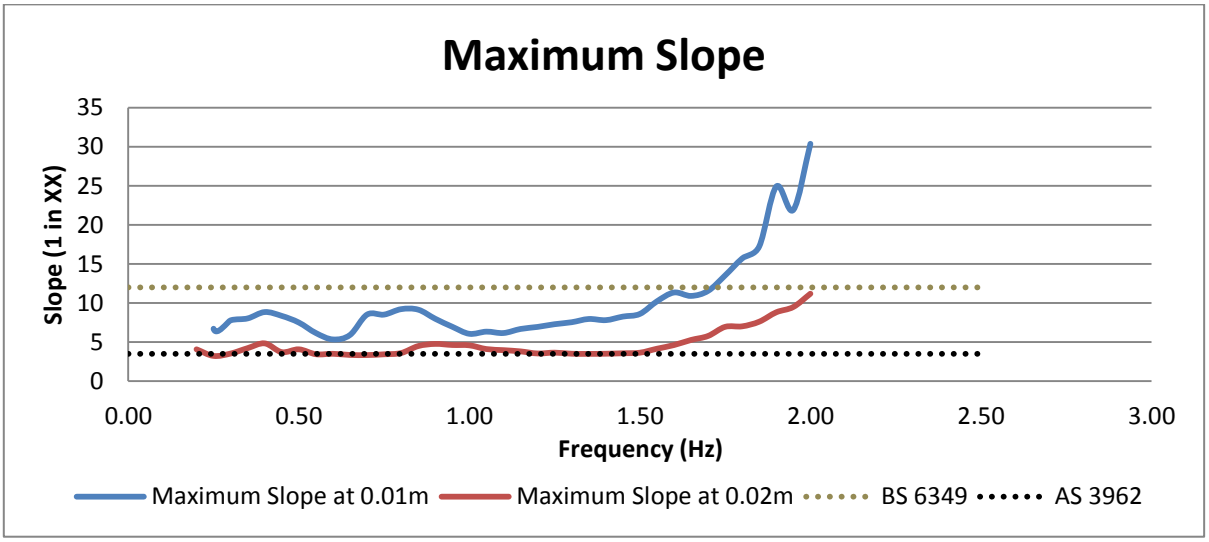

Figure 6.2 - Pontoon Slope compared to Guideline Slopes

6.5.2 Model Pontoon Response

The pontoon is easily able to operate under the guidelines set out by the Australian Standards. The pontoon can operate safely within the guidelines by British Standards only when the amplitude of waves is 0.02m. The gradient of the pontoon is too great to be considered suitable for use under all but the lowest frequency values tested when waves have amplitude 0.01m. As these standards refer to a gangway or linkspan any specified gradients may be misleading values to attempt to adhere to, as such the slopes given cannot be given too much credence.

As no specific gradient for a modular pontoon could be found, this report suggests that instead a compromise is taken between these standards and for the case of a modular pontoon a maximum allowable gradient of 1 in 7.5m be achieved. This allows the occasional maximum gradient to be suitable for use; the average gradient would be expected to be significantly more gradual than this. This gradient would

suggest that the pontoon tested within this project would be at the limit of its safe operating capacity across the duration of the 0.01m amplitude waves.

This maximum allowable gradient should be used as a guideline only, as being based on a limited range in data, it may not be generalisable to different wave conditions. This could be explored should further research be conducted to refine this maximum allowable gradient.

7 Conclusion

This project set out to investigate the relationship between the movement response of a modular pontoon system and the characteristics of the waves which it is subjected to. In addition to this to explore the gradient the surface of such a modular pontoon would reach under this same wave conditions.

By identifying and understanding these key relationships, modular pontoons, which are being used increasingly more often in industry, can be used with more assurance as to their suitability for their situation. This also allows existing modular pontoon and pier to be managed more effectively if used in adverse wave conditions as the limits of when this pontoon can be considered safe for use will have been identified.

The study determined that in terms of the movement response of a modular pontoon to waves a simple relationship is followed. As one would expect, waves with greater amplitudes will result in greater movement from the modular pontoon than waves with smaller amplitude. Additionally, it was determined that in general as the frequency of the induced waves is increased, the movement response exhibited by the modular pontoon is reduced. This movement refers to the magnitude of the change rather than the rapidity of said movement. Using differential calculus, the rate of change of the surface level of the modular pontoon could be an area to explore in further testing.

The study also determined that wave breaking had a confounding effect upon the movement of the modular pontoon and directly contradicts the previously stated relationships. When wave breaking is present the motion of the modular pontoon system is greater than what would be expected based upon the amplitude of the wave. This is an important factor which needs to be taken in account when used in real world applications; consequently, testing to explore the reaction of a modular pontoon with an emphasis on breaking waves would be a valuable contribution towards the field.

Additionally, this study explored the gradient that was reached by the surface of the modular pontoon. The findings from this investigation revealed that with higher wave amplitudes higher gradients were reached by the pontoon. It was also discovered that frequency has a reduced effect upon the slope of a modular pontoon when in the low frequency wave range. As waves with higher frequencies are encountered by the modular pontoon system the slope reach becomes rapidly more gradual. It is suggested that for modular pontoon systems being deployed under conditions similar to those modelled that a maximum allowable gradient of 1 in 7.5m be considered and that care is taken when utilising modular pontoon when in more severe wave conditions than those modelled.

To summarise the points made above, under low frequency waves the gradient of a modular pontoon is drastically more severe than when under higher frequency waves. In addition, significantly more movement is seen when low frequency waves are encountered. It is clear that these lower frequency waves pose the biggest threat towards the functionality and suitability for use of a modular pontoon system.

Acknowledgements

I would like to thank Dr Martyn Hann for his valuable and constructive comments and suggestion during this work. His readiness to give up his time so generously has been very much appreciated.

I would also like to extend my gratitude towards the technicians of the Marine Building, without whose help; this project would likely not have been completed.

Finally, I wish to thank my family and friends for their support and encouragement throughout the project.

References

Abul-Azm, A.G. and Gesraha, M.R. (2000) 'Approximation to the hydrodynamics of floating pontoons under oblique waves', *Ocean Engineering*, 27(4), pp. 365–384. doi: 10.1016/s0029-8018(98)00057-2.

Australian Standards (2001) *AS 3962—2001 Guidelines for design of marinas*. Sydney: Standards Australia International.

British Standards Institution (2007) *BS 6349-8:2007 Maritime structures. Code of practice for the design of Ro-Ro ramps, linkspans and walkways*. London: British Standards Institution.

Buckingham, E. (1915) 'The Principle of Similitude', Nature, 96(2406), pp. 396–397. doi: 10.1038/096396d0.

Chanson, H. (1999) *Hydraulics of open channel flow: An introduction: Basic principles, sediment motion, hydraulic Modelling, design of hydraulic structures*. London: Butterworth-Heinemann.

Chanson, H. (2004) *Environmental hydraulics for open channel flows*. Oxford: Elsevier Butterworth-Heinemann.

GeoData Institute (2016) *Channel coastal observatory*. Available at: http://www.channelcoast.org/ (Accessed: 26 April 2016).

Gesraha, M.R. (2004) 'An eigenfunction expansion solution for extremely flexible floating pontoons in oblique waves', *Applied Ocean Research*, 26(5), pp. 171–182. doi: 10.1016/j.apor.2005.05.002.

Gao, R.P., Wang, C.M. and Koh, C.G. (2013) 'Reducing hydroelastic response of pontoon-type very large floating structures using flexible connector and gill cells', *Engineering Structures*, 52, pp. 372–383. doi: 10.1016/j.engstruct.2013.03.002.

Gottschalk, L. and Krasovskaia, I. (2002) 'L-moment estimation using annual maximum (AM) and peak over threshold (POT) series in regional analysis of flood frequencies', *Norsk Geografisk Tidsskrift - Norwegian Journal of Geography*, 56(2), pp. 179–187. doi: 10.1080/002919502760056512.

Hamill, L. (2011) *Understanding hydraulics*. 3rd edn. Basingstoke: Palgrave Macmillan.

Hughes, S.A. (1993) *Physical models and laboratory techniques in coastal engineering*. Singapore: World Scientific Publishing Co Pte.

Iglesias, G. (2016) *Long Term Wave Statistics (A statistical study of rare events)*[PowerPoint presentation]. COUE318: Coastal Engineering Design and Analysis. Plymouth University.

Kamphuis, J.W. (2010) *Introduction to coastal engineering and management*. 2nd edn. Singapore: World Scientific Publishing Company. In-line Citation: (Kamphuis, 2000)

Kan, W. (no date) *Motion in the sea -- waves*. Available at: http://www.marine.tmd.go.th/marinemet_html/lect18.html (Accessed: 14 February 2016).

Le Mehaute, B. and Webb, L.M., 1964. Periodic gravity waves over a gentle slope at a third order of approximation. *Coastal Engineering Proceedings*,*1*(9).

Loukogeorgaki, E., Michailides, C. and Angelides, D.C. (2012) 'Hydroelastic analysis of a flexible mat-shaped floating breakwater under oblique wave action', *Journal of Fluids and Structures*, 31, pp. 103–124. doi: 10.1016/j.jfluidstructs.2012.02.011.

Michailides, C., Loukogeorgaki, E. and Angelides, D.C. (2013) 'Response analysis and optimum configuration of a modular floating structure with flexible connectors', *Applied Ocean Research*, 43, pp. 112–130. doi: 10.1016/j.apor.2013.07.007.

Plastics technical properties (no date) Available at: http://www.dotmar.com.au/density.html (Accessed: 16 January 2016).

Reeve, D., Chadwick, A. and Fleming, C. (2011) *Coastal engineering: Processes, theory and design practice*. 2nd edn. New York: Taylor & Francis.

Shibayama, T. (2008) *Coastal processes: Concepts in coastal engineering and their application to Multifarious environment*. Singapore: World Scientific Publishing Co Pte.

Silvester, R. (1974) *Coastal engineering, Vol. 1: Generation, propagation and influence of waves*. United Kingdom: Elsevier Science.

Schwartz, M.L. (1984) *The encyclopedia of beaches and coastal environments*. Edited by Maurice L. Schwartz. Netherlands: Kluwer Academic Publishers.

Versadock: Modular Docking solutions (2016) Available at: http://versadock.com/ (Accessed: 12 November 2016).

Wiegel, R.L. (1964) *Oceanographical Engineering*. Prentice-Hall, University of Michigan.

Wood densities (no date) Available at: http://www.engineeringtoolbox.com/wood-density-d_40.html (Accessed: 15 January 2016).

Appendices for this work can be retrieved within the Supplementary Files folder which is located in the Reading Tools menu adjacent to this PDF window.